UNIVERSITAT POLITÈCNICA DE VALÈNCIA

ESCUELA TÉCNICA SUPERIOR INGENIEROS INDUSTRIALES VALENCIA

TRABAJO FIN DE MASTER EN CONSTRUCCIONES E INSTALACIONES INDUSTRIALES

Condition Assessment of Critical Industrial Infrastructure with Low-Cost, Battery-Powered, Efficient Wireless Intelligent Sensors (LEWIS)

AUTHOR: MARLON FRANK AGÜERO INJANTE

SUPERVISOR: FERNANDO MOREU

Academic year: 2017-18

To my parents, my brother and my sister, thank you for always supporting my dreams.

ACKNOWLEDGEMENTS

Completing this thesis wouldn't have been possible without the help, support, and guidance of so many people, and I would like to express my gratitude to all of you. I would like to thank Dr. Moreu for his guidance and support, professionally as well as personally. I also wish to thank Dr. Ali Ozdagli for guiding me through my work and for being in my thesis committee. Furthermore, I am grateful to all my colleagues and friends at the Smart Management of Infrastructure Laboratory (SMILab): Dilendra Maharjan, Philipp Weisterman, Emmanuel Ayorinde, and many others.

Finally, I would like to especially acknowledge the financial support I received from Pronabec, who funded my graduate studies in Spain, and the Technical University of Valencia, who funded my exchange program at the University of New Mexico. It was a privilege to conduct the research presented in this thesis with their financial assistance.

ABSTRACT

Engineers and managers have recently started exploring the use of sensors for monitoring of critical loads and operations in the field. In particular, the application of wireless sensors (WS) has gained interest due to their cost reduction advantages when compared to their wired counterparts. Many new advances have made the development of cost-, labor-, and time-effective WS for collecting data, as a result of which WS can now be used even more reliably to make informed decisions about the performance of structures under service and extreme loads. Apart from the cost benefits, wireless devices have many other advantages: they guarantee real-time interactions with events; they do not require human attendance on site, and they are less invasive for structures (see Now et al. (2017) for a detailed overview). While many of the challenges for efficient WS have been solved by sensor systems, such as low-cost, real-time, efficient wireless intelligent sensors (LEWIS), there are several issues in the application of such sensors for remote applications, including the high data collection rate and their limited ability for Outdoor Environment Monitoring (OEM, which refers to monitoring environmental conditions such as humidity, temperature, water leakage, and water pressure). This thesis presents the testing and implementation of a second generation low-cost, battery-powered efficient WS (LEWIS2) that can measure and record acceleration as well as angular velocity in real time. This new sensing platform operates on the basis of an open-source Arduino ecosystem, and it combines low-cost, battery-powered microcontrollers with affordable wireless transmission modules and accelerometers. The intended LEWIS2 system has been developed to transmit the data in real-time either to the base station or if necessary, to a remote office via an internet connection. The first application of LEWIS2 describes the result of the field experiments that were conducted by the author of this thesis in order to validate the effectiveness of the proposed new LEWIS2 sensor for outdoor and remote sensing applications. The field experiment involved he launch of a rocket. Furthermore, during the experiment The author of this thesis was able to monitor the trajectory of one rocket. This information can collect structural responses during launch to inform the structural design of future launches. Thus, the experiment not only shows that the new LEWIS2 system can be used for outdoor applications, but that it can be also applied to new disciplines such as aerospace engineering. This proves the flexibility of the LEWIS2 platform. The second application that this thesis focuses on is displacement. Displacement of structures under potential disturbances is widely regarded by industrial infrastructure inspectors and managers as vital diagnostic in the condition assessment and the evaluation of performance. However, existing procedures for measuring displacements in industrial infrastructures are often time-consuming and costly. The low-cost, battery-powered efficient wireless intelligent sensor (LEWIS2) proposed in herein is able to measure acceleration and angular velocity in the three axes to estimate the reference-free dynamic displacements of structures under potential disturbances. The effectiveness of the new LEWIS2 system has been evaluated through a series of laboratory experiments. First, displacements measurements from the field reported in Moreu et al. (2015) were applied to a shake table in which a column was placed. Then the author of this thesis excited the proposed LEWIS2 platform, and we referenced the LVDT displacement sensor. It was possible to obtain transverse displacements in the column with LEWIS2, which were then compared with the displacements received from LVDT. The results of the laboratory experiments show that the system tested by the author of this thesis has the capacity to accurately reconstruct transverse displacements of structures and to transmit the data wirelessly in real-time. These experiments indicate that the LEWIS2 platform described in this work can be adopted for the performance assessment of structures in a cost-effective and yet accurate way. More generally, the LEWIS2 system developed in this thesis can significantly improve the efficiency of SHM of many civil structures, industrial constructions, and installations.

Keywords: Low-cost, wireless, sensor, acceleration, structure, displacement, outdoor, monitoring, industrial constructions, installations.

INDEX

CHAPTER 1. METHODS AND PROCEDURES OF STRUCTURAL HEALTH MONITORING (SHM)

This chapter provides the motivation for the research undertaken in this thesis. The general aim of this thesis is to develop a new method for assessing the condition of critical industrial infrastructure, which makes use of low-cost, efficient wireless intelligent sensors (LEWIS). The underlying reason why such methods are developed is the fact that all civil engineering structures deteriorate and may become damaged. This process occurs as a result of aging, intensive use, heavy loads, or disasters such as earthquakes and flooding. This chapter outlines the technological methods, commonly termed Structural Health Monitoring (SHM), which are utilized so as to maintain and monitor civil infrastructures and to detect potential damage as early as possible. The efficiency of Structural Health Monitoring procedures is important for many reasons: it improves overall public safety, reduces costs related to maintenance of infrastructure, and provides longer life spans to structures.

This chapter has the following organization. Sections 1.1 - 1.2 provide a general description of the problem of decay and aging of civil structures in the USA. Sections 1.3 - 1.7 introduce the concept of Structural Health Monitoring and overview its procedures, components, as well as challenges for its reliable application. Subsequently, section 1.8 addresses displacement measurement, which is an aspect of SHM that is important for the topic of this thesis.

1.1. Industrial Infrastructure

Efficient and reliable industrial infrastructure is the backbone of the economy in every country in the world. Infrastructure components, such as bridges, dams, tunnels, airports, and high-rise towers are the critical ingredients for ensuring both the economic strength of each nation and safety for all human beings. Thus, they are critical for the public's welfare, security, and prosperity.

All infrastructure components deteriorate due to the natural process of aging. Moreover, they may experience deterioration and damage because of heavy utilization as well as unexpected environmental events, such as earthquakes, hurricanes, and flooding. If infrastructure components are not properly maintain and fail, the results may bring severe economic consequences and crucially, they may also lead to the loss of human lives. Examples of such disasters include the fall of the Tacoma Bridge in US (1940), Seongsu Bridge in South Korea (1994), Sampoong Department Store in South Korea (1995), Nicoll Highway in Singapore (2004), Minnesota Bridge in US (2007). They are shown in **Figure 1-1** to **Figure 1-5**.

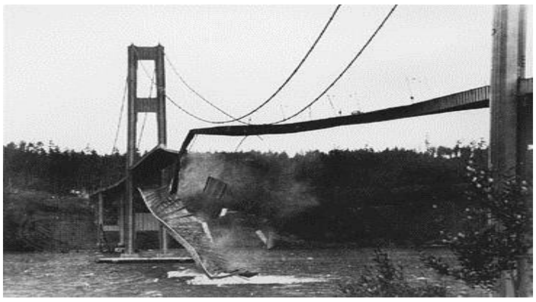

Figure 1-1. Tacoma Bridge in US (1940).

Figure 1-2. Seongsu Bridge in South Korea (1994).

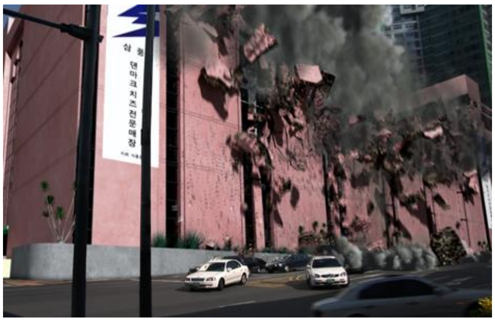

Figure 1-3. Sampoong Department Store in South Korea (1995).

Figure 1-4. Nicoll Highway in Singapore (2004).

Figure 1-5. Minnesota Bridge in US (2007).

1.2. US Industrial Infrastructure Decay

According to the report card compiled by the American Society of Civil Engineers (ASCE) in 2017, the US infrastructure is in an appalling state. The majority of the infrastructure in the USA was awarded a grade of D or less in the report, with an overall average grade of D+, on the scale from A to F (ASCE, 2017). The findings of the report are consistent with the evaluations that were carried out in the preceding decade, which also reviewed the US infrastructure very poorly (see (ASCE, 1988), (ASCE, 1998), (ASCE, 2001), (ASCE, 2005), (ASCE, 2009), (ASCE, 2013), (ASCE, 2017)). **Table 1-1** summarizes the American infrastructure grade performance over the last decades.

Table 1-1. US infrastructure grade performance 1988 – 2017 (ASCE 1988, 1998, 2001, 2005, 2009, 2013, 2017).

Year	1988	1998	2001	2005	2009	2013	2017
Roads	C+	D-	D+	D	D-	D	D
Bridges	-	C-	C	C	C	C+	C+
Transit	C-	C	C-	D+	D	D	D-
Aviation	B-	C-	D	D+	D	D	D
School	-	F	D-	D	D	D	D+
Railways	-	-	-	C-	C-	C+	B
Waterways	-	-	D+	D-	D-	D-	D
Energy	-	-	D+	D	D+	D+	D+
Dams	B	D	D	D	D	D	D
Cumulative	**C**	**D**	**D+**	**D**	**D**	**D+**	**D+**

To give an example, National Protection and Programs Directorate published a report on "Aging and Failing Infrastructure Systems: Highway Bridges" see OCIA (2016) on September 14, 2015. According to this report, there are approximately 600,000 highway bridges in the United States. The average age of bridges in the United States is 42 years, whereas most highway bridges are designed for a life of approximately 50 years. Even though many newer bridges are designed to last 75 years or more, the majority of the bridges will have outlived their designed lifespan within the next 10 to 40 years. In consequence, in 2013 the American Society of Civil Engineers assigned a grade of C+ to the American bridges.

The Report states that it is possible to extend the life of a bridge past its intended lifespan with appropriate maintenance, preservation measures, and regular inspections. Admittedly, bridge conditions have been steadily improving, though the funding for highways and highway bridges may be insufficient and inadequate to maintain the current capacity. Although obsolete or structurally deficient bridges are not necessarily unsafe, they may require more frequent maintenance or it may be necessary to impose restrictions on speed, load, size, and the number of vehicles permitted on these bridges. Such measures may in turn lead to traffic congestion on other bridges, increase distance, travel time, and fuel consumption. Once structurally deficient bridges become unsafe, they must be removed from service, which has severe economic consequences. Importantly, even though the lifespan of a bridge can be extended through repairs, they may in the end become too costly, and as a result of the lack of prior appropriate maintenance, such a bridge must be closed and replaced.

Given the findings of the reports quoted above, appropriate maintenance and repair of the infrastructure components must become a priority. The maintenance procedures need to be appropriately designed, and civil engineers and managers require reliable methods for data acquisition so as to be able to make informed decisions about the safety and maintenance prioritization (for a detailed discussion, see Moreu (2015)). The subsequent sections of this chapter describe the ways in which such decisions are made in the procedures related to Structural Health Monitoring.

1.3. Definition and the motivation for the application of structural health monitoring systems

Structural health monitoring system (SHM) is a term that was first used in structural engineering in the late 1980's (Boller, Fou-Kuo, & Yozo, 2009). It is understood in the literature as the application of an on-site, non-destructive sensing mechanism whose role is to analyze the structural properties of a construction. The purpose of SHM is to determine whether damage has occurred, and in case it has occurred, to establish its location, evaluate its severity, and determine whether the damage has consequences for the residual life of the construction (Silkorsky, 1999).

The areas in which SHM has been applied changed in the history of engineering. The emergence of the SHM methods in the 1980's is attributed to an increased interest in the structural health of offshore petroleum platforms and the condition of aerospace structures. Subsequently, SHM procedures have been developed in conjunction with development and cost and size reduction of digital computing hardware and sensors (see Doebling, et al. (1996)

and Sohn, et al. (2004)). These days SHM is a popular and well-established research field in civil engineering.

There are two major approaches to SHM. On the one hand, SHM may be based on the application of models that examine physical properties of the structure under investigation. On the other hand, SHM may be also based on machine learning or statistical examination of the data observed in the analyzed structure (Farrar & Worden, 2007).

1.4. The procedure of performing Structural Health Monitoring (SHM)

The overall procedure of performing Structural Health Monitoring consists in identifying possible damage to a structure. Damage is understood as an undesired modification of the material and/or its geometric properties, which results in faulty current state and potentially inappropriate structure performance in the future. Therefore, in order to detect damage, it is necessary to apply appropriate devices, such as sensor systems and compatible software and hardware facilities to monitor the operational environment and the performance of the examined structure. Since structural health may deteriorate either at a normal aging speed or undergo unexpected failure when affected by violent events such as earthquakes, different procedures must be applied in the respective circumstances. Thus, long-term SHM requires regular monitoring of a structure over time, during which samples of structural responses are collected periodically, coupled with operational environment measurements that are received from sensors. Furthermore, additional data is investigated, related to the capacity of a structure to perform its designated functions as well as the degree of its expected degradation that is a consequence of aging. These types of data are then analyzed in order to give an accurate evaluation of the current state of a structure and to make predictions about its future performance (Farrar, et al., 2003). Conversely, SHM applied to structures that have been affected by a violent, unexpected event such as an earthquake or a tornado requires different procedures, which focus on the integrity of the structure and the determination of its current reliable performance.

Irrespective of whether SHM is a long term procedure or whether it is applied to in the aftermath of a violent event, its objectives can be divided into five levels. These levels were proposed by Farrar et al. (2009) and are reported here following Chen (2018b).

1) Level I - damage detection, which provides a qualitative indication that a structure may have been affected by damage;
2) Level II - damage localization, which gives information concerning the likely location of the damage;
3) Level III - damage classification, which specifies the type of the damage that has been detected;
4) Level IV - damage assessment, which gives an estimate of the damage extent;
5) Level V - damage prognosis, which provides an estimate of remaining useful life of a structure and the safety of is application

The five levels quoted above represent a gradual increase in knowledge about the damage state of an examined structure. Thus, it is necessary to have access to information about a lower level (such as damage localization) in order to draw conclusions or predictions about the higher level (such as damage classification or assessment). Furthermore, each level may require distinct operational procedures and methods to be applied. For instance, damage detection and localization can be established through an application of vibration-based damage detection methods that come from structural dynamic response measurements; the type of damage is determined through a correlation of the measured data with the data from structures that display a specific kind of damage, whereas the fourth and fifth levels are achieved through the application of analytical models (Chen & Ni, 2018b).

Each of the levels of SHM may require applying different procedures, depending on the structure under investigation and the type of damage involved. For example, Chen and Bicanic (2000), Chen (2008) and Chen and Maung (2014) point out that global damage of large civil structures can often be successfully evaluated with the application of vibration-based identification methods. These methods comprise two types of techniques: data-based and model-based techniques. The former technique applies measurements directly so as to provide an evaluation of the current state, and its detection results are limited, as it may only establish the existence of damage. The latter technique is more powerful, as it both locates and assesses damage in the structure. However, it depends on baseline data, as it requires a validated initial physical model of a structure. This requirement may be problematic when it is necessary to perform global modal assessment, given that vibration measurements from the undamaged, initial structure may have been influenced by environmental conditions, for instance by wind and temperature. Therefore, such conditions need to be taken into account during the assessment.

Even though the first SHM level, damage detection, represents the lowest level of knowledge about damage and only presents general information about the existence of damage or strength degradation, it is nevertheless very advantageous if it is interpreted as an early safety warning. Furthermore, if the SHM system is automated, the damage detected at the first level may provide information about parts of structure that need to be examined for safety, which may be extremely beneficial if the affected areas are inaccessible and may have been neglected during earlier visual inspections (Cross, Worden, & Farrar, 2013).

1.5. The components of a Structural Health Monitoring system

A Structural Health Monitoring system consists of two major subsystems: the monitoring subsystem, which examines a structure through a network of sensors, and the evaluation subsystem, which feed information provided by interpretation algorithms. These two subsystems, in turn, consist of many subcomponents, such as sensors, devices for data acquisition, transmission, processing, and management; as well as mechanisms for health evaluation and decision making. To ensure successful and reliable monitoring, each of the subcomponents must function properly, as each of them is responsible for a different part of the monitoring procedure. Thus, in order to secure a reliable sensing mechanism, it is necessary to provide an appropriate number and types of sensors, which must be mounted in designated locations. The component that deals with data acquisition must be equipped with hardware that selects the excitation methods, provides signal conditioning, as well as stores acquired data. The data must then be efficiently transmitted via wireless or wired networks, whereas the data processing unit must be capable of providing data validation, normalization, fusion, cleansing, and compression. Finally, the obtained data must be securely stored and managed so that the final health assessment is accurate.

An overall scheme of health monitoring procedure is presented in **Table 1-2** (see Chen (2018b) as well as Wong and Ni (2009) for an application of the scheme to the structural health monitoring of bridges.

Table 1-2. Overall scheme of health monitoring procedure.

Observation	This stage includes, collecting, processing, analyzing, and reporting the observed and measured data, derived from the sensory systems.
Evaluation	This stage may comprise performance analyses of the structures that are being monitoring in real-time or near real-time, as well as off-time diagnostic and prognostic examinations of the structures during a regular operation or following an extreme event, such as an earthquake.
Rating	This stage includes ranking and prioritization of the structural components; it is meant to plan and schedule subsequent inspection and/or maintenance actions.
Management	This stage involves regular storage and rapid retrieval of all the data meant for observation, evaluation, and rating, with a view of future further analysis.

1.6. The advantages of applying a Structural Health Monitoring system

Since the principal purpose of applying Structural Health Monitoring systems is to ensure safety, the most basic benefit of such systems is averting danger to human life. However, even though the application of SHM procedures involves an increased cost that needs to be borne, SHM has a number of direct advantages for structural engineering. Thus, as pointed out by Ko and and Ni (2005), Frangopol and Messervey (2009), and summarized by Chen (2018b), SHM greatly enhances the design as well as management of structures. First, it provides vital information about performance of civil engineering structures, as it records the behavior of structures in different environmental conditions, such as temperature, the strength of wind, and load resistance. On the basis of these data, it is possible to implement performance-based designs. Furthermore, a detailed analysis of the performance of structures may provide information about anomalies related to excess load or faulty response, which in turn may be used to accurately establish performance thresholds. Second, the findings of SHM may be used to introduce or validate assumptions about design and parameters, which has the advantage of potentially enhancing design guidelines and specifications for structures of a related type that will be developed in the future. In this regard, SHM also gives an opportunity to improve the accuracy of structural assessments that are normally performed by giving access to recorded structural response data, which can be readily analyzed. Third, SHM is advantageous for scheduling performance assessments: the necessary periodical inspections can then be carried out “as required,” when instructed by the monitoring data. What is more, it is then possible to implement real-time safety assessments in all types of circumstances, during both normal operations as well as immediately after extreme events and disasters such as earthquakes. Fourth, SHM provides a substantial economic benefit, as it gives access to more accurate performance information, which can be then used to determine the suitable time for repair and scheduled maintenance.

SHM is a vital procedure because of the nature of civil engineering structures, which in contrast to cars or aircraft are not constructed with the same degree of precision. Furthermore, there are many variables surrounding the construction of civil engineering projects. As noted by Chang et al. (2003), the structure of some materials used in civil engineering such as concrete is never uniform, and it may affect the behavior of structures, together with environmental factors such as moisture and temperature. For example, the temperature variation between the main land and the sea or river may give rise to special thermal effects around bridges, which in turn may have an impact on the natural frequencies of bridges. Apart from the environmental issues, the ultimate mechanical behavior of a civil structure is influenced by ground conditions and various constraints that occur on the construction site. Furthermore, it may also be affected by the quality of workmanship, which if happens to be poor, the physical properties of a structure may differ from the original design. The possibility of the occurrence of all these factors means that the physical model of a structure based on the idealized behavior of its components may be not attained in practice. This fact is an additional challenge for the appropriate implementation of SHM, but it also points to the importance of reliable SHM procedures.

Still, as was pointed out earlier, SHM has numerous safety benefits and may also bring substantial financial savings. As a practical illustration of the advantages provided by the application of SHM strategies, Chen (2018b) gives an example routine inspection and maintenance of bridges. Like most other civil constructions in the USA, bridges must be regularly inspected, which happens every two years. This type of periodic inspection may be problematic if SHM rules are not followed. Namely, if any unexpected damage occurs to the bridge outside the time of scheduled inspections, it may be left unnoticed and cause safety hazard. Conversely, it may be the case that the inspections are scheduled more frequently than practically required, so their performance may bring about an unnecessary financial expense, especially when they involve routine replacement of some structural components even if they are in excellent working condition. Both of these issues are solved when reliable SHM methods are applied. Maintenance then becomes continual and condition-based (see Cross, et al. (2013), quoted in Chen (2018b)), with an added benefit that any downtime that structures may potentially be affected by becomes reduced.

The application of SHM strategies also brings advantages on a conceptual level. As Chen (2018b) observes, it allows us to better understand structural responses and develop new codes, which may lead in turn to the implementation of comprehensive, all-round methodologies for automated inspections and eventually, to a completely condition-based monitoring and maintenance (see also Karbhari (2009)). In a long run SHM will provide more detailed and accurate diagnostics concerning the prediction of the remaining life of structures, their most advantageous repair planning, as well as efficient mechanisms for data analysis in real time.

In more general terms, the application of SHM may give more robust performance data, which in turn will provide us with better understanding of structural responses. In consequence, this may lead to a creation of more refined and fine-tuned methodology of structural design and ultimately, general innovations in the area of both the design as well as maintenance of engineering structures.

1.7. Challenges for structural health monitoring systems

The previous subsection described the benefits of applying SHM. However, since SHM is still a relatively novel area in civil engineering, it has not been completely worked out yet and some of the problems concerned with the efficient implementation of SHM remain a challenge.

In general, the primary reason for implementing SHM is to ensure safety. As Boller (2009) observes, this is frequently problematic because when a new structure or a device becomes constructed for a particular purpose, it may be difficult to predict how the material that has been used for this particular structure will react in a new environment, in new operating conditions, or how it will interact with other components of the structure. Furthermore, the more unfamiliar the operational conditions of a new structure, the higher safety factor needs to be applied.

Appropriate implementation of SHM can be a serious challenge. This is due to the fact that although all civil engineering structures age and deteriorate, the deterioration occurs due to a multitude of factors. Some of these factors are related to the regular process of material aging, wear and tear, but many other factors cannot be easily predicted or accounted for. For instance, structures may age more rapidly because of inclement weather events and general environmental concerns, which may accelerate the process of steel corrosion and concrete carbonation. Since weather patterns are relatively stable in a given climatic area, the speed and type of weather-related damage can be estimated. Correspondingly, under normal conditions it is possible to estimate within a high degree of probability the effect of operational factors on the structural health of a construction, such as the impact of regular vehicle traffic on a bridge structure, on the assumption that the traffic volume is relatively constant over long periods of time. However, it is considerably more difficult to assess structural health of structures that have been subjected to infrequent events of extreme strength, such as an earthquake or a tornado, as these events are "variables with uncertainties" (Chen & Ni, 2018b). The occurrence of such events is virtually impossible to predict. In consequence, engineering structures that have been affected by those events may have unexpectedly aged beyond their design life, and as a result, they are prone to display premature deterioration and subsequent performance problems.

Furthermore, Brownjohn et al. (2011) point out that the structures that were affected by such infrequent, violent events require rapid and reliable condition assessment. This is a problematic issue, as noted by Chen (2018b), given that the condition assessments of many civil constructions such as bridges heavily rely on visual inspections. This type of inspection is regarded as inaccurate and subjective, therefore more reliable and effective methods should be implemented.

A number of challenges for SHM are related to the way this system could be implemented and function in practice. They have been discussed at length by Farrar and Lieven (2007) as well as Farrar et al. (2009), and they are summarized here following Chen (2018b).

Thus, an issue that is a challenge for SHM that must be addressed in the future is the fact that in many instances it is necessary to perform feature selection as well as damage detection when data coming from a damaged system is not available. Furthermore, SHM should be sensitive enough to detect damages of a small size, such as fatigue cracks. This may be a challenging issue given that large and sophisticated civil structures contain many components, and they may have experienced multiple damages. Furthermore, SHM systems may be quite selective when it comes to types of damage detection, so in the case of complex structures, some SHM systems may only detect certain areas of damage. Correspondingly, some types of damage may only occur and accumulate following an extended period of time. This is a serious issue for SHM sensing systems, as they need to operate and continuously provide reliable and repeatable measurements for a long period of time. Consequently, these systems must be sufficiently accurate and robust.

Another challenge for the sensing systems in SHM is that they need to be preselected before actual field deployment, and that they must be taken care of so that they do not become damaged during service. The selection of sensors could be a complex procedure, as it is necessary to specify their correct number and location so as to also leave room for certain redundancy in the network. The sensors should also be inexpensive and easy to mount in the structures.

Furthermore, since civil structures operate in different and changing environmental conditions, the sensors and response measurements should be appropriately fine-tuned so that they do not report temperature and moisture variations as indications of structural damage. For instance, variation in moisture may lead to a change in the mass of concrete, whereas temperature changes may have an effect on the stiffness of a structure. Such environmental and operational conditions should be taken into account so that they are not mistaken for damage by the sensing systems.

Finally, there are also a number of technical challenges which must to be addressed. SHM methods are frequently multi-disciplinary, so they require remarkable technology integration and engineers with broad and diverse technical expertise.

CHAPTER 2. METHODS OF DETECTING AND MEASURING DISPLACEMENT - LITERATURE REVIEW

The previous chapter has described general aims and methods of Structural Health Monitoring (SHM). In order to apply SHM successfully and efficiently, it is necessary to apply reliable mechanisms. This chapter addresses methods that are used to detect and measure displacement. It begins with an overview of a number of current contact and non-contact methods, pointing out their benefits and potential disadvantages. Subsequently, it discusses Wireless Sensor Networks (WSNs), whose importance as a displacement measurement method has increased recently due to their reliability and low costs associated with their installation and maintenance.

2.1. Methods of Measuring Displacement in Industrial Infrastructure

Displacement is a type of structural response of a civil structure, and it is understood as the distance from which an element (a column, a frame, or a beam) moved with respect to its original position. It can be measured in terms of distance as well as in terms of rotation.

As pointed out by Chen and Ni (2018a), displacement may affect dynamic as well as quasi-static components. The displacement of dynamic components may be triggered by wind, seismic activity, and vehicular loading, whereas the quasi-static components may be affected by thermal effects, variation in static loading and settlement.

Measuring displacement can be a complex process because displacements frequently involve relative values, for which it is necessary to define a reference datum. Displacements are normally established with respect to an undeformed or unloaded state. There are many methods that can be applied for measuring displacement. In the case of dynamic displacements caused by vibrations, it is possible to compute them from accelerations by double integration following high pass filtering. Other techniques of measurement used for calculating displacements include both traditional survey methods and more advanced techniques (Catbas, Kijewski-Correa, & Aktan, 2012). Chen and Ni (2018a) list the following methods applied for computing displacement, which will be addressed in more detailed in the subsequent sections: (i) laser and LED devices, such as laser Doppler vibrometers (LDVM); (ii) GPS (global positioning system); (iii) image tracking through CCD arrays; (iv) surveying and total station; (v) optical marker tracking; (vi) microwave interferometry, such as radar system; (vii) pneumatic system; (viii) contacting displacement measurements, including LVDT.

2.1.1 Laser and led devices, including Laser Doppler Vibrometers (LDV)

As explained by Garg (2018) following Polytec (2017), Laser Doppler Vibrometer (LDV) relies on the principle of interferometry. The transverse target displacement is established through the interference of reference and reflected beam, which causes light and dark pattern. The light emitted by the LDV becomes split into a reference beam and a measuring beam. Given that the distance covered by the reference signal is at all times constant within the vibrometer assembly, it can be applied to compute the movement of the target. The measuring beam is transmitted from the vibrometer and becomes reflected by the target. The frequency of the reflected signal is altered due to the target movement, whereas the reflected signal triggers an interference pattern with the reference signal. The process is sketched in **Figure 2-1**, following Garg (2018), who attributes the **Figure 2-1** to Polytec (2017).

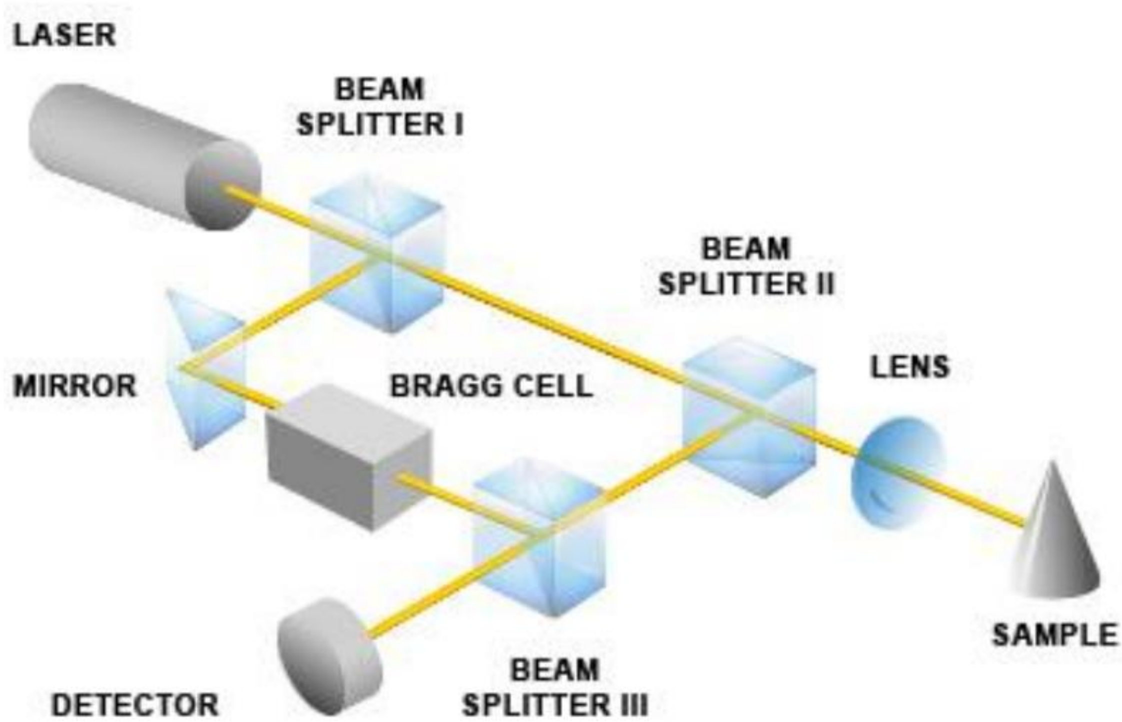

Figure 2-1. Working of a Vibrometer (Polytec Inc., 2017) from Garg (2018).

Laser and LED devices can be used in dynamic testing of bridges for displacement and velocity measurements. They have some strong advantages, such as the fact that their outputs occur real-time and do not require significant post-processing, and that they are not hindered by inclement weather conditions or low visibility (Mehrabi, 2006). However, the application of LDVMs is restricted given that they cannot perform simultaneous measurement of multiple locations (Chen & Ni, 2018a). Moreover, they require a surface close to the target and are not reference-free displacement sensors (Garg, 2018).

2.1.2 Global Positioning System (GPS)

Global positioning system (GPS) is a contact sensor that has been successfully applied to compute displacement in oscillating flexible civil engineering structures, including high-rise buildings, dams, long suspension bridges, and for seismic and land slide applications. It has also been used to derive their modal frequencies, normally up to 1 Hz (Psimoulis, Stella, Dimitris, & Stathis, 2008); (Ni, 2014). However, for some measurements it is necessary to use high frequency GPS receivers.

GPS systems have a number of unique advantages over other sensors and play an increasingly important role in SHM. As pointed out by Cranenbroeck (2015), GPS systems provide high accuracy of measure, do not require inter-visibility between measuring points, and can be applied in inclement weather conditions. Furthermore, they also are capable of measuring at high rates with low latency, over long baselines, and they have a long service life. Still, Chen and Ni (2018a) observe that although GPS receivers are a promising sensing technology, as they can produce measurement giving the accuracy rate of a few millimeters at sample rates that are as high as 20 Hz, they are still rather costly to operate. Furthermore, Garg (2018) notes that the readings provided by GPS units may not be accurate enough for identifying minor displacements, such as the ones triggered by train crossing events on railway bridges. To circumvent this issue and increase accuracy, Kogan et al. (2008) and Moschas and Stiros (2013) combined GPS-captured measurements with data retrieved from accelerometers and inertial measurement units (IMU), though as observed by Garg (2018), this type of setup may require installation in the field, which is not always possible.

2.1.3 Image tracking via CCD Arrays

Image-processing-based displacement measurements, which make use of a high-speed camera for the structural health monitoring and a computer analysis system, are capable of rapidly assessing conditions of structures such as bridges and improve their reliability with high accuracy, as in the case of an experiment at the Vincent Thomas Bridge in California reported in Wahbeh et al. (2003). Thus, Jo et al. (2018) propose a Computer Vision-Based Bridge Displacement Measurement method, which includes three components: a marker, a smartphone camera, and a computer equipped with image processing software. It involves three main stages: (i) motion image acquisition, (ii) image processing for object tracking, and (iii) calculation of bridge displacement, provided in **Figure 2-2**.

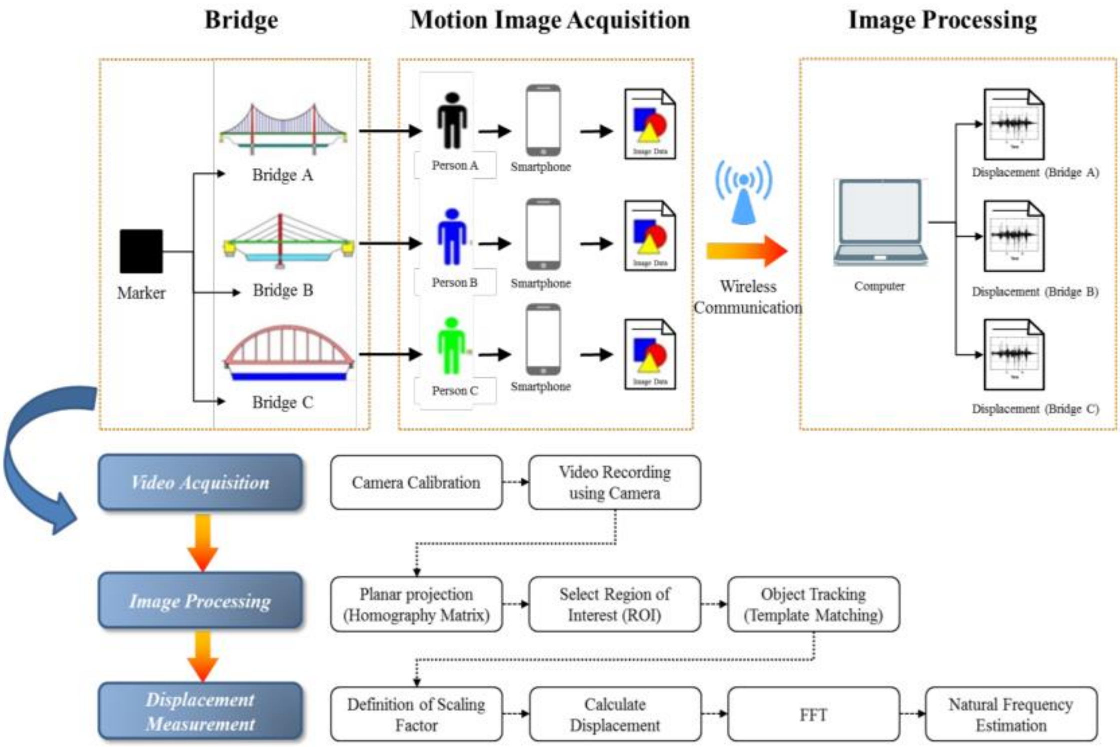

Figure 2-2. The scheme of a Computer Vision-Based Bridge Displacement Measurement method, taken from Jo et al. (2018).

However, as pointed out by Jo et al. (2018), a problematic issue with this method is the fact that in comparison to other sensor systems, computer vision-based systems need large-capacity servers for storing both data and images for the long-term monitoring. Furthermore, the quality of displacement data obtained may be severely impacted by the camera performance and image processing algorithms, whereas vibrations in the area around the camera may trigger noise, leading to potential errors.

2.1.4 Surveying and Total Station

Total stations have been applied to calculate the movement of structures, such as tunnels and bridges, as well as natural processes, such as deformation of the land in landslide regions. Total stations involve using remote systems that log measurements several times per day via a modem, subsequently statistical tests are applied to confirm if the points have moved. **Figure 2-3** provides an example of the application of a total station for the monitoring of The Gorgopotamos Bridge, a railroad bridge constructed in 1905, situated near Lamia, a town located in central Greece, approximately 150 km North-West of Athens. The Gorgopotamos bridge is 211 m long and has a maximum height of around 32 m. The **Figure 2-3** comes from Psimoulis and Stiros (2013).

Figure 2-3. Gorgopotamos Railway Bridge and the robotic total station in the foreground.

The **Figure 2-3** shows the robotic total station that was applied for the measurements in the foreground; the inset presents the prismatic reflector with a GPS antenna located on top of it, which is set on the handrail of the bridge.

As reported in Cosser et al. (2003), the advantages of the total station systems include high accuracy and the possibility of conducting measurements indoors and in urban canyons, which are inaccessible to GPS systems. The usage of total stations has also disadvantages, such as low sampling rate, problems with measurement reliability in adverse weather conditions, and the fact that a clear line of sight between the prism and the total station is required.

2.1.5 Microwave Interferometry (Radar Systems, Light Detection and Ranging (Lidar) and LDV)

Microwave interferometry, for example radar systems, can be used for remote detection of structural displacements in dynamic and static tests of large constructions, such as bridges. The system is based on an interferometric radar, which is capable providing images with a sampling rate that is sufficiently high to track the movements of structures. The radar identifies a differential displacement of the target in its cone of view through the exploitation of the phase information of the back reflected microwave signal, as shown in **Figure 2-4** to **Figure 2-6** following Pieraccini (2013)

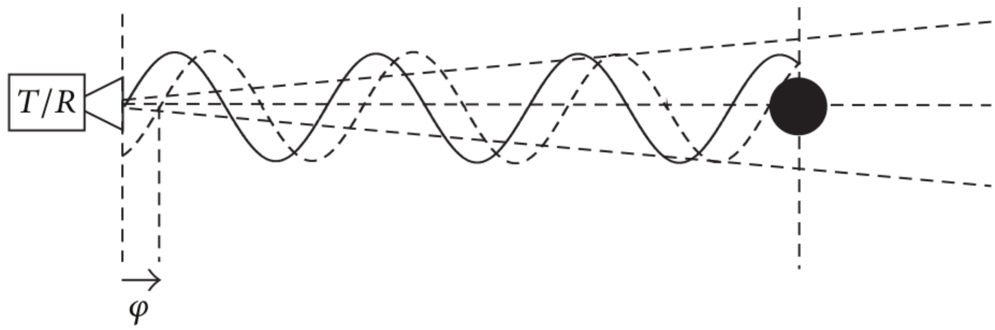

Figure 2-4. Working principle of interferometry T/R: transmit/receive equipment, f: phase from Pieraccini (2013).

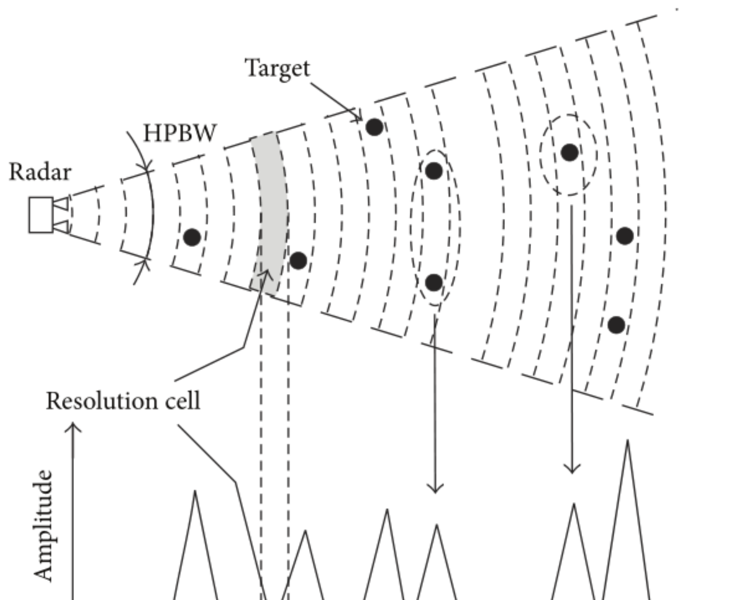

Figure 2-5. Interferometric radar. HPBW: half-power beam width from Pieraccini (2013).

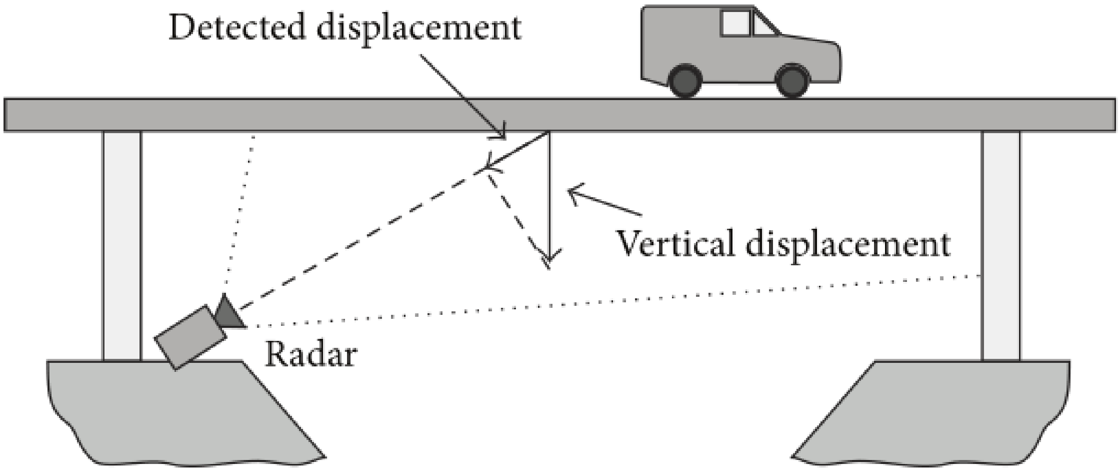

Figure 2-6. Interferometric radar for monitoring a bridge from Pieraccini (2013).

Pieraccini (2013) points out that a major advantage of such systems is the fact that they can detect small displacement at great distance. Because of this property, they are used for testing the conservation status of large historic and ancient monuments, for example Giotto's tower in Florence (Pieraccini, Fratini, Parrini, Pinelli, & Atzeni, 2005) and the Leaning Tower of Pisa (Atzeni et al. (2010)). They are also applied for dynamic monitoring of larger structures, such as bridges.

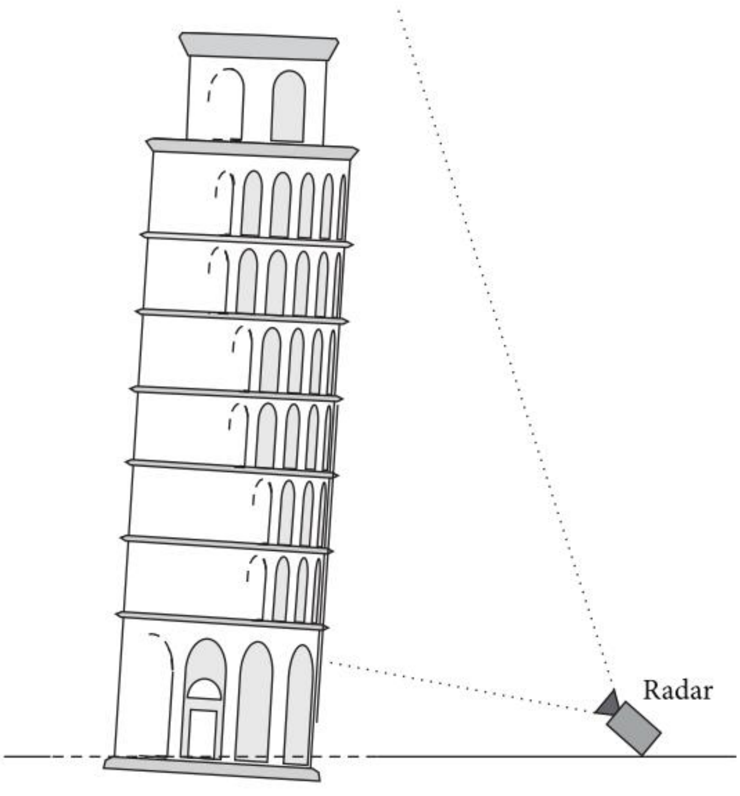

Figure 2-7. Radar measurement of Leaning Tower of Pisa from Pieraccini (2013).

Pieraccini et al. (2006) further observes that as in the other systems of non-contact monitoring, a strong advantage of microwave interferometry is the fact that it avoids the use of costly scaffolding, and that structures, such as bridges, can be continuously used during the monitoring process. Microwave interferometry systems, however, also have serious drawbacks, such as the fact that any elements, such as trees or scaffolds located between the sensor and the structure under investigation can falsify the measurement results. Furthermore, these systems are only capable of detecting the displacement component along the line-of-sight direction of the radar, and are not capable of detecting torsional effects of structures or providing a bidimensional map of the displacement. In consequence, they are predominantly used for monitoring structures that have a prevalent dimension, such as towers (which span in vertical direction) and bridges (which span in horizontal direction).

2.1.6 LVDT and other contacting displacement measurements

Linear variable differential transformers (LVDTs) are contact sensors that operate on the principle of a transformer, using a primary coil as the AC excitation source and two secondary coils, as shown in **Figure 2-8** following Figliola & Beasley (2010).

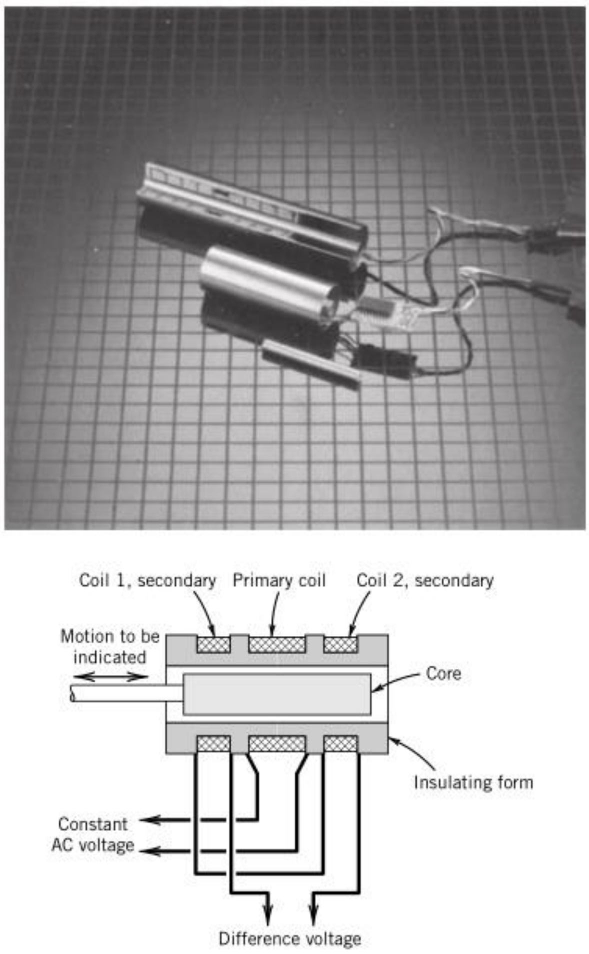

Figure 2-8. Construction of a linear variable differential transformer (LVDT). (Figliola & Beasley, 2010).

The coil assembly is usually placed on stationary forms, and the core becomes attached to the object, the position of which is being computed. The coil assembly comprises three coils of wire, which have been wound on a hollow form. The core of permeable material slides without obstruction through the center of the form. The inner coil functions as the primary, and it becomes excited by the AC source. The magnetic flux triggered by the primary is coupled to the two secondary coils, and induces an AC voltage in each of the coils (Dunn & Davis, 2018).

LVDTs are widely used in many applications, including civil engineering structures as well as power turbines, nuclear reactors, aircraft, and satellites. They are very robust sensors, and if they are properly used, they may have a virtually infinite cycle life. They can be applied under high vibration and shock levels, in harsh environments, and potentially they may operate at very high temperatures, up to 1200 °F (650 °C).

However, the usage of LVDTs in civil engineering structures such as bridges can be a challenge. As shown by Moreu et al. (2014), the application of LVDTs to compute transverse bridge displacement under dynamic train loading is problematic. First, it is time-consuming to attach the sensors to bridges each time a test is run. Second, mounting the sensors to bridges that span large areas, such bodies of water deep gorges, can be costly and challenging.

There are a number of other methods for measuring displacement, such as pneumatic systems and optical marker tracking. Since each method has different advantages and limitations, sometimes two different methods are combined, which provides more accurate measurement results and helps overcome signal deficiencies, as in the experiment reported by Moschas et al. (2013), which combines Robotic Total Stations with GPS sensors for dynamic monitoring of the Gorgopotamos train bridge in Greece. In such a scenario, the advantage of using the GPS system is the fact that it records higher frequency oscillations though it has a small signal-to-noise ratio in low-amplitude oscillations, whereas Robotic Total Stations record small amplitude, lower-frequency oscillations with considerably higher signal-to noise ratio. Alternatively, it is also possible to derive displacements from other measurements, including strain, acceleration, velocity, and rotation signals (Chen & Ni, 2018a).

2.2 Wireless sensor networks (WSNs)

This section provides a description and general characteristics of wireless sensor networks. In this way it serves as a background for the case study and an analysis of the LEWIS2 sensor, which is provided in chapters 3 and 4.

Wireless sensor networks (WSNs) have received increased attention recently because of their numerous advantages and overall technological potential in structural health monitoring in comparison to wired sensor networks. These advantages are briefly discussed in this section, following Noel et al. (2017) review paper.

First, a substantial merit of WSNs is the fact that they are very economical. Each wireless sensor node costs approximately USD 500. By comparison, the cost of wired sensor networks is very high, ranging between USD 10,000 and USD 25,000 (Cao & Liu, 2012). Thus, the application of WSNs leads to severe cost reductions, which allows both short-term structural monitoring as well as more extensive monitoring of public and private infrastructure. This in turn permits earlier damage detection, less frequent routine inspections, increase of the lifespan of many structures, and better public safety in general.

Second, another advantage of WSNs concerns their deployment time, which is very short and may take as little as half an hour. By contrast, the deployment time of wired sensors is considerably longer, and in some cases it has been reported to take several days (Chintalapudi, K. et al., 2006). The lifespan of WSNs is typically lower than that of wired sensors, and is usually limited by node battery lifespan. In the case of wired sensors, the lifespan is longer, usually constrained by hardware lifespan.

Third, the low cost of WSNs makes it possible to increase the number of sensors mounted on structures and in consequence perform more thorough and reliable monitoring. The number of WSNs is typically higher than the number of wired sensors also due to the ease of their installation. The fact that there are more WSNs, deployed at various locations in the structure, has a side-effect of the amount of collected data being considerably higher than in wired sensors, with higher sensing and sampling rates. This high data collection rate may pose a challenge for the network design. In consequence, it is necessary to apply suitable data aggregation and processing. Furthermore, since the data from WSNs is relayed over wireless connections, sensor synchronicity is of a higher concern than in the case of wired sensors.

To conclude, this chapter has addressed a number of different methods of measuring displacement in industrial infrastructure. It discussed their advantages and disadvantages and showed the ways they can be successfully employed in structures. Special attention has been paid to Wireless Sensor Networks, which show significant benefits over other displacement measurement systems. Specifically, their low installation and maintenance costs as well as high reliability have made them a very strong alternative to the other existing systems. The subsequent chapters will describe a powerful low-cost wireless sensor LEWIS2 and demonstrate how it can be successfully applied for detecting and measuring displacement.

CHAPTER 3. LOW-COST, BATTERY-POWERED, EFFICIENT WIRELESS INTELLIGENT SENSOR (LEWIS2) FOR OUTDOORS AND REMOTE SENSING APPLICATIONS

3.1. Introduction

During the recent years, wireless sensors (WS) have been widely used in a variety of applications concerned with water monitoring (Lee, Banerjee, Fang, Lee, & King, 2010), (Perez, et al., 2011), (Jiang, Xia, He, & Wang, 2009), forest monitoring (Bayo, Antolín, Medrano, Calvo, & Celma, 2010), (Yunus, Ibrahim, & Özgür, 2012), industrial monitoring (Silva, Guedes, Portugal, & Vasques, 2012), (Zhao, 2011), aerospace monitoring, agriculture monitoring (Raul, et al., 2008), (Li, Deng, & Ding, 2008), battlefield surveillance (Qian, Sun, & Rong, 2012), (Padmavathi, Shanmugapriya, & Kalaivani, 2010), intelligent transportation (Tacconi, Miorandi, Carreras, Chiti, & Fantacci, 2010), (Tubaishat, Zhuang, Qi, & Shang, 2009), smart homes (Lee, Wu, & Aghajan, 2011), (Bangali & Shaligram, 2013), animal behavior monitoring (Handcock, et al., 2009), (Nadimi, Jørgensen, & Christensen, 2012), and disaster prevention (Bahrepour, Meratnia, Poel, Taghikhaki, & Havinga, 2010), (Lacono, Romano, & Marrone, 2010).

Outdoor environment monitoring (OEM) is of principal importance in civil engineering for the purpose of both protecting human life and avoiding economic loss due to structural disasters. Its main aim is to ensure that buildings, infrastructures, and lifelines operate at a high of level of performance and do not incur damage. Wang, Lynch, & Sohn (2014) and Chang, Flatau, & Liu (2003) point out that in recent decades SHM has become increasingly important. First, structures in urban areas are subject to unprecedented demand because of the growth in population and transportation, which gives rise to a higher level of deterioration of structures. The deterioration occurs at a faster pace than before. Thus it is becoming more difficult to provide replacement in a timely manner. In consequence, an increasing number of structure components start to exceed their designated life spans and become more costly to maintain. Second, due to the process of climate change, building and infrastructure are more frequently affected by natural disasters, such as tropical storms and flooding, as witnessed during Hurricane Harvey in Houston in 2017 and earlier during Hurricane Katrina in New Orleans in 2005 (Eamon, Fitzpatrick, & Truax, 2007), (Padgett, et al., 2008), (Chen, Wang, & Zhao, 2009). In consequence, it is becoming increasingly important to develop systems of sensors which allow us to establish how structures behave under normal and extreme load conditions. Sensors are important devices for engineers, as they permit observations of infrastructure to an unprecedented level of detail. In a long run, these observations can be used by engineers to optimize system designs and improve maintenance operations. (Spencer, Sandoval, & Kurata, 2004)

As was pointed out in Chapter 2, with the increased demand for sensor systems, the application of wireless sensors (WS) has recently gained considerable attention due to the cost reduction advantages and the possibility of performing high-density installation, which targets local damage, and provides more detailed and reliable information about the dynamic properties of the structures. In consequence, new advances have been made in the development of WS to offer an economical method for collecting data that can be applied to make informed decisions about their dynamic performance as well as its trajectory, which is important for aerospace engineering because it allows the optimization of the structural design of aerospace infrastructure, such as rockets (see section 3.4 below). Apart from the cost benefit, WS have a number of other conceptual advantages: they guarantee reliable interactions with events, they provide real-time access to vital information, they do not require human attendance on site, they permit quick decisions, and in general they make monitoring less invasive for structures. In this way wireless devices overcome the challenges of many other systems of monitoring (see the discussion in chapter 2). Moreover, since remote monitoring includes a wide variety of applications, WS can be used to complement wired systems by decreasing the costs of wiring, maintaining efficient power applications, and permitting development of new types of measurement applications (Lynch J. P., 2012), (Lynch & Loh, 2006).

However, in spite of the recent developments and the advances in the research on WS, there are several issues and challenges in the application of WS that require further attention. For instance, the high data collection rate of WS for monitoring pose serious network design challenges. Moreover, the cost of using WS is still too high. The challenges for efficient WS have been solved by an efficient, low-cost, real-time wireless intelligent sensing (LEWIS) system that has been developed to monitor critical infrastructure. The effectiveness of LEWIS has been verified by a series of laboratory experiments reported in Ozdagli et al. (2018), and this chapter relies on the findings of that study. Nevertheless, the application of LEWIS remains problematic when it is used outdoors and for remote applications. The main challenges are the high data collection rate of WS, their high cost, and their limited ability for Outdoor Environment Monitoring (OEM).

Therefore, building on the laboratory experiments and the findings presented in Ozdagli et al. (2018), the author of this thesis conducted field experiments to validate the effectiveness of the new LEWIS2 for outdoor and remote sensing applications. In order to validate the versatility of LEWIS2, the field experiment focused on the trajectory of one rocket. In this way it was possible to demonstrate that LEWIS2 is applicable not only to infrastructures in civil engineering, but also in aerospace engineering, such as the optimization on the structural design of rockets.

The results of the field applications have clearly shown that the proposed system can be used for outdoor applications. This chapter presents a report on the findings of the experiment, and it offers the following contributions: (1) it provides the design of a low-cost, battery-powered efficient WS (LEWIS2) that can measure angular velocity and acceleration measurements in real time, which are important parameters in many applications, and (2) it offers the field validation for the effectiveness of the new LEWIS2 with an additional application: rocket trajectory. The results of the field applications indicate that the proposed system can measure angular velocity, acceleration to accurately estimate the trajectory of different applications. In conclusion, the platform can be used for outdoor applications, including a rocket trajectory and the vibration on the tower of a tramway under traffic operations.

This chapter also proposes (see section 3.5 below) further modifications that may be carried out in the future to improve the characteristics of LEWIS2. They involve the use of an enclosure and solar panel for outdoor applications, including measuring vibrations of a car in a cable tramway, vibrations on a tall tower under operations. More generally, the final objective of the research presented in this chapter is to contribute to OEM capabilities for multiple field environments and structural responses of diverse infrastructures with low-cost, efficient wireless intelligent sensors.

3.2 Low-Cost, Battery-Powered, Efficient Wireless Intelligent Sensor (LEWIS2)

3.2.1 Wireless Sensor Node Elements

Generally, a wireless sensor node is made of the following essential parts (Akyildiz, Su, Sankarasubramaniam, & Cayirci, 2002): sensor, microcontroller, external memory, transceiver, and power source. The sensor or sensing unit acquires data from the field and converts the analog data into digital data. The microcontroller is used as a processor to acquire and process the sensor raw data to store the results to an external memory. The external memory may save a large amount of data, enabling posterior access by the user and remote sensing abilities. The transceiver unit enables sharing data between other wireless nodes and the base station. The final element is a power unit which consists of an energy source (capacitor, battery, or both of them). Depending on application requirements, additional units can be added. **Figure 3-1** presents the way these elements are interconnected.

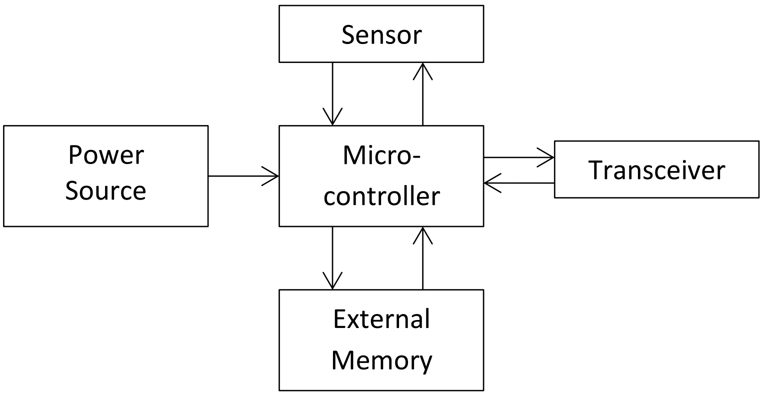

Figure 3-1. Interconnection of basic components of a wireless sensor.

3.2.2 Elements of the proposed LEWIS2

The previous section outlined the key components of wireless sensors. The present section will present recommendations of specific components that could be provided for LEWIS2 on the basis of their characteristics and availability on the market. By means of summary, the elements of the proposed LEWIS2 are given in **Figure 3-2**. Additionally, **Table 3-2** shows a cost summary of the elements of LEWIS2, with a description of each element.

3.2.3 Microcontroller

Arduino Uno R3 is an open-source microcontroller board, based on the ATmega328P microcontroller. The board contains the following components: 14 digital input/output pins (which is used to read information from the sensor and to control the actuator, respectively), six of which can be applied as PWM outputs), 6 analog inputs, a USB connection, a power jack, a 16 MHz quartz crystal, an ICSP header, and a reset button (Arduino, 2018). It can be powered from AC adapters, most USB chargers, or the USB port through a computer.

Arduino Uno R3 features a number of components intended for communication with a computer, another Arduino board, or other microcontrollers. It works together with Arduino

Software (the Arduino Integrated Development Environment (IDE)), and it can ran online and offline.

Arduino Uno R3 has numerous advantages. It is flexible, features a user-friendly interface, and enables smooth communication between devices (Banzi, Massimo, & Shiloh, 2015).

3.2.4 Sensor

LEWIS2 employs a multi-chip module (MCM) MPU9250, produced by SparkFun Electronic. The MPU9250 is a multi-chip module that comprises two dies that are integrated into one QFN (Quad-Flat No-leads) package. One of the dies contains a 3-Axis accelerometer together with a 3-Axis gyroscope, whereas the other die contains an AK8963 3-Axis magnetometer manufactured by Asahi Kasei Microdevices Co. All the components are housed in a small 3x3x1mm package, which in consequence means that MPU9250 is the smallest 9-axis Motion Tracking device available worldwide. MPU9250 has low power consumption, which makes it a very economical device (Invensense, 2018).

3.2.5 Transceiver

3.2.5.1 Arduino Wireless SD Shield

Arduino Wireless SD Shield, produced by Arduino, is a device that performs two functions. First, it permits the Arduino board to perform wireless communication via a wireless module, in particular, the XBee transceiver module, but it can be also used with other modules that have the same footprint to form mesh networks. Second, it features a micro SD socket, which permits accessing and storing large amounts of data. It also contains an on-board switch, which enables the wireless module to communicate with the microntroller or with the USB-to-serial converter, and a perfboard grid that can be used to prototype the user’s circuit (Arduino, 2018). Perfboard (DOT PCB) is a material used to prototype electronic circuits. It has the form of a rigid, thin sheet, with holes pre-drilled at regular intervals across a grid. The holes are ringed by square or round copper pads.

The micro SD socket included in the Arduino Wireless SD shield can be interfaced with the Arduino SD library. The two functions of the shield (storing and accessing data and interfacing with XBee transceiver modules) can be utilized independently or together. The shield is user-friendly and improves the capabilities of the Arduino board.

3.2.5.2 XBee Series 1 Module

XBee Series 1 Module is a very simple and reliable device that permits communication between computers, systems, microcontrollers, and which also supports point to point and multi-point networks and is and convertible to a mesh network point. The XBee module has the range of 100 feet indoors and 300 feet outdoors with line-of-sight. It is very easy to set up and no prior configuration is required to operate it in peer to peer environments, which means that it can replace wired serial connections that were formerly used. The module is equipped with a wire antenna of excellent quality.

According to Digi XBee documentation (2018), the XBee Series 1 Module offers the following characteristics: Its indoor/urban range is up to 100 ft., and the outdoor RF line-of-sight range is up to 300 ft. The transmit power output is 1 mW (0dbm) and 2 mW (+3dbm); the RF Data Rate is 250 Kbps; the Receiver Sensitivity-92dbm. The supply voltage is 2.8 – 3.4 V; the idle/receive current is typically 50 mA (@ 3.3 V), whereas the power-down current is 10 uA. It operates on the frequency of ISM 2.4 GHz, in the temperature ranging from -40 to 85 C. The antenna options are PCB, Integrated Whip, U.FL, RPSMAPCB, and it has 16 direct sequence channels, with filtrations PAN ID, Channel & Source/Destination.

3.2.5.3 XBee Explorer

XBee Explorer is an USB to serial base unit that can be applied in the Digi XBee line. The unit is very simple to use and is compatible with all the XBee modules, which include the standard and Pro versions of the Series 1 and Series 2.5.

XBee Explorer houses an FT231X USB-to-Serial converter, which translates the data between the XBee and the computer. It also contains a reset button, a voltage regulator to provide power to the XBee, RSSI (signal-strength indicator), power indicator, and four LEDs that are helpful for debugging the XBee. To operate an XBee, it must be plugged into the XBee Explorer, and connected via a mini USB-cable to a computer of a cellphone. This gives direct access to the serial and programming pins located on the XBee unit (XBee Explorer, 2018).

3.2.6 Power Source

Nanotech 1.0 Battery was used as the power source. The battery has the specifications showed in the **Table 3-1**.

Table 3-1. Specifications of Nanotech 1.0 Battery.

Capacity	1000mAh
Voltage	2S1P / 2 Cell / 7.4V
Discharge	25C Constant / 50C Burst
Weight	60g (including wire, plug and case)
Dimensions	71x35x12mm
Balance Plug	JST-XH
Discharge Plug	XT60

This battery makes use of modern LiPo nano-technology substrate, which leads to higher discharge rates and a lower voltage sag in comparison to traditional non nano-tech lithium polymer batteries of a similar density, and gives more power under load. Other benefits of nanotech 1.0 batteries include lower internal impedance, which can reach 1.2mO, in comparison to 3mO of a standard battery, and better thermal control, which does not exceed 60degC. Their life cycle may almost double that of standard lipoly technology batteries (Nanotech, 2018). These properties make it a reliable battery that can be used to provide energy to the wireless sensor, so that it can work in an autonomous way.

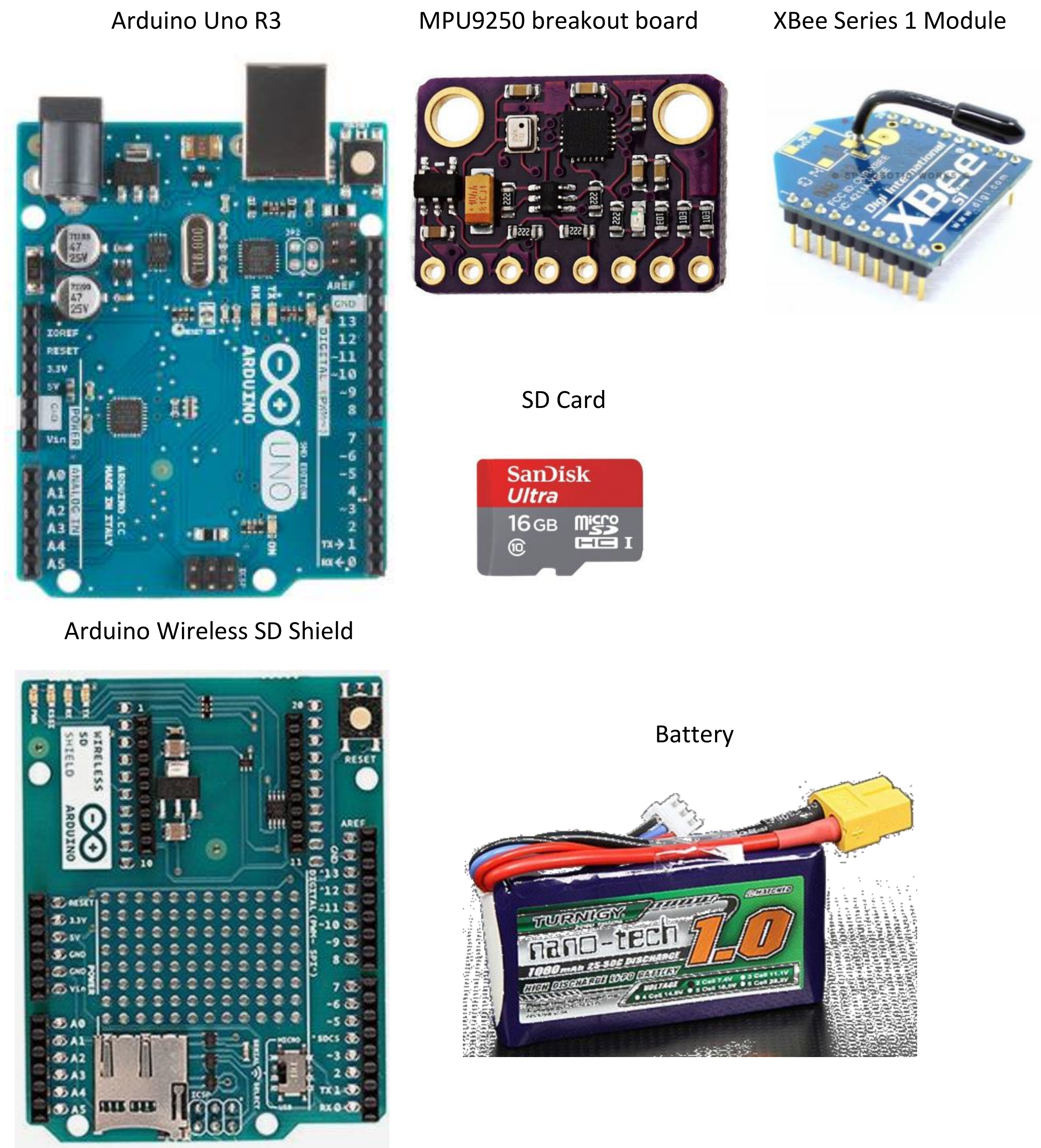

Figure 3-2. Components of the Arduino-based LEWIS2.

3.2.7 External Memory

The SD card uses Arduino Wireless SD shield; in the LEWIS2 communication proceeds via the microcontroller. The communication between the microcontroller and the SD card uses SPI (Serial Peripheral Interface).

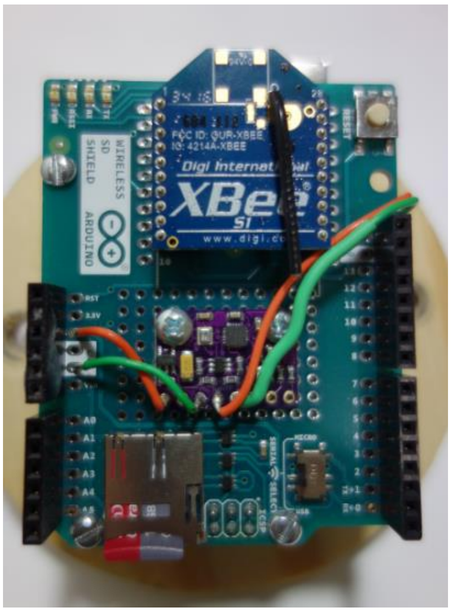

Figure 3-3. Assembled LEWIS2.

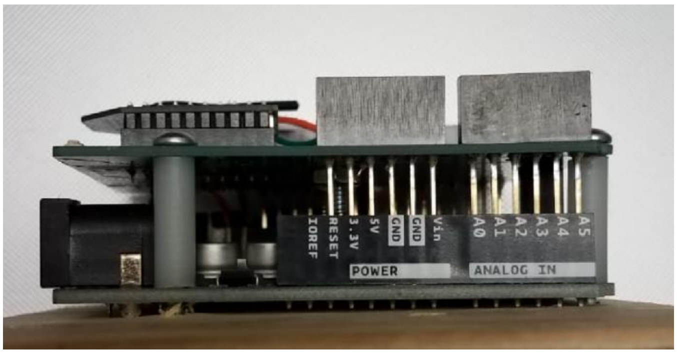

Figure 3-4. Assembled LEWIS2 – side view.

Table 3-2. Essential sensing platform components LEWIS2.

Element	**Description**	**Price, $**
Arduino Uno R3	Microcontroller	$4.00-$25.00
MPU9250	Sensor	$9.99
XBee Series 1 Module	Wireless transmission module	$25.00
Arduino Wireless SD Shield	Communication XBee S1 Module and Arduino Uno R3	$15.00
Battery	Battery Nanotech 1.0	$6.33
SD Card	SanDisk Ultra 80MBs MicroSD Memory Card - 16GB	$10.00
	Total	**$70.35 - $91.35**

3.3. Trajectory Estimation with LEWIS2

As was pointed out in the previous sections, LEWIS2 has numerous advantages: it has a small size, it is very economical, and it does not need much power. LEWIS2 can provide information about acceleration and angular velocity. On the basis of these data it is also possible to draw informed conclusions about trajectory. However, a crucial issue in the extraction of information from accelerometers and gyroscopes, which so far has not been completely solved, is the fusion of the noisy data they produce. This problem is sometimes addressed through the application of Kalman filters or their non-Gaussian versions, nonlinear variants to estimate the attitude and in consequence, also the position (see, for example, Bistrovs & Kluga (2012), Fischer et al. (2013), and Ligurio et al. (2013)). However, since they require sampling rates and large state vectors, the application of such filters is not a viable solution for low-cost sensors that use batteries of limited-capacity. A promising fix that has been applied recently is a low-cost, low-computation complementary filter as the algorithm to estimate the attitude (see, for example, Zhi (2016)). It can be used with heuristic drift elimination methods, which have been demonstrated by Zhi (2016) to almost completely remove the drift triggered by the gyroscope and in consequence, it generates a highly precise, drift-eliminated estimate of altitude and position, as shown in **Figure 3-5**, following Zhi (2016).

In line with Zhi's (2016) procedure, the author of this thesis uses an algorithm with the steps listed below in order to obtain trajectory while applying LEWIS2:

Step 1: We pass the data of accelerometer and gyroscope to an explicit complementary filter (ECF). The filter provides us with output quaternions for the complete series of data. The attitude that we wish to obtain can be represented by quaternions or by their transformation into some other rotation representation. When the Matlab code is applied, the quaternions become transformed into rotation matrix and produce 3D-trajectory monitor animations.

Step 2: We apply the quaternion that was computed in step 1 in order to have the accelerometer data rotated from the sensor frame to the Earth frame.

Step 3: We integrate the acceleration in Earth frame received in step 2 in order to obtain velocity in the earth frame.

Step 4: The accelerometer data is passed to the Zero Velocity Update (ZUPT) filters (which include a first-order Butterworth low-pass filter and a first-order Butterworth high-pass filter) in order to obtain the processed magnitude of acceleration and to determine stationary periods.

Step 5: The stationary periods are applied to zero-update the velocity that was computed in step 3 in order to obtain ZUPT velocity in the Earth frame.

Step 6: The drift occurring during the non-stationary periods is removed because of integration.

Step 7: We perform integral on linear velocity that was computed in step 6 in order to obtain the position in the Earth frame.

Step 8: The position data is passed to Enhanced Heuristic Drift Elimination (EHDE) in order to obtain the estimation of the drift eliminated position in the Earth frame.

Once these steps are followed, attitude estimation is obtained from step 1, whereas drift eliminated displacement is rendered by step 8 (see Zhi (2016)).

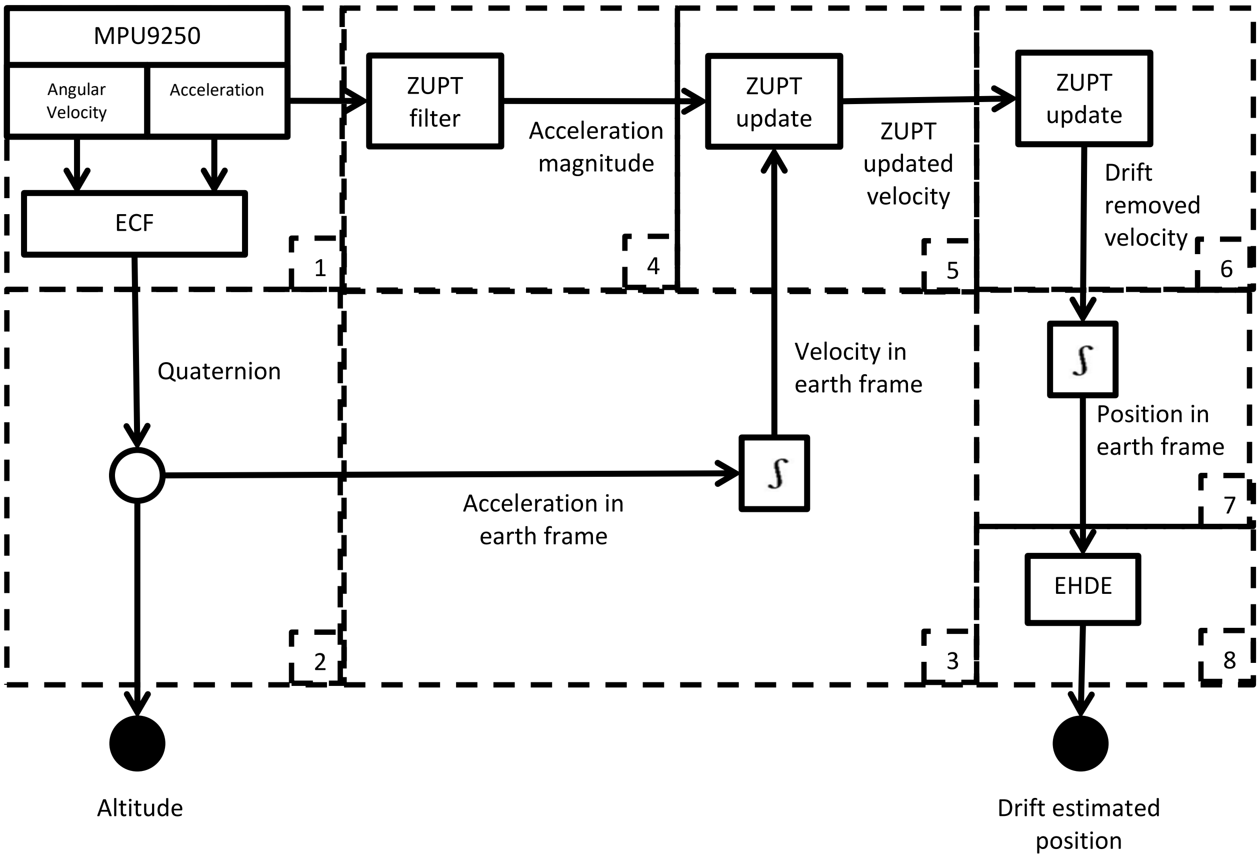

Figure 3-5. Steps to obtain trajectory with LEWIS2.

Significantly, drift reduction techniques are applied within each integral level. Thus, in the level of acceleration, gyro drift becomes reduced through the implementation of ECF with a PI controller. In the level of velocity, integral drift of acceleration is reduced thanks to the implementation of ZUPT. In the level of displacement, the drift triggered by small errors coming from two lower levels which became integrated into a larger drift becomes removed through the implementation of the EHDE.

3.4. Field Validation

Rocket Trajectory

The aim of the experiment reported in this section was to test the functionality of the LEWIS2 and to determine whether LEWIS2 can accurately record the acceleration and angular velocity and to estimate the trajectory of the rocket during its flight. Through the analysis of the acceleration (see **Figure 3-10**) and angular velocity data collected from the launch (see **Figure 3-11**), we tested how effectively the low-cost wireless sensor could quantify the launch events (see **Figure 3-12**). To accurately visualize the acceleration and angular velocity during takeoff, researchers recommend a measuring frequency of 500 Hz (Sutton & Biblarz, 2010).

The rocket that was used to launch the LEWIS2 sensor was a small, partly self-constructed, hobby-style rocket named the Raptor. The rocket was 0.1 m in diameter, 2.2 m long, and weighed approximately 5.2 kg with the motor and the sensor within the rocket. The sensor was located 1.8 m from the base of the rocket. The motor propellant weighed 0.6 kg and the motor burned for 7.6 s. After the launch, when the motor burned out, the entire rocket weighed approximately 4.6 kg. The type of motor used for the launch was the Aerotech J135W, which contained “White Lightning” propellant.

Once the sensor was integrated into the rocket (see **Figure 3-6**), the rocket was placed on the launch rail. The rocket was mounted vertically on a launch rail where it was attached firmly to prevent it from launching too early. At this point, we activated data acquisition wirelessly using XBee explorer connected to a smartphone, sending instructions wirelessly to the LEWIS2 via the XBee Series 1 Module component (see **Figure 3-7, Figure 3-8**), and the rocket was then raised in the vertical position awaiting launch. During the experiment we established that the XBee antenna transmitter had to be located within about 3 feet of the LEWIS2 sensor for successful activation. On completing the launch protocol, which specifies the procedures that must be followed, the rocket was launched. At apogee, the parachutes were deployed, and the rocket returned to the ground safely. Data acquisition on the sensor was stopped after the rocket was retrieved (see **Figure 3-9**). The accelerations and angular velocities during takeoff and travel were correctly stored on the memory card.

Due to the high measuring frequency, it was possible to precisely record the acceleration and angular velocity during takeoff to provide the final estimate of the rocket trajectory (see **Figure 3-13**).

Figure 3-6. Placement of the wireless sensor inside of the rocket.

Figure 3-7. Activation of the wireless sensor remotely to record the acceleration and angular velocity.

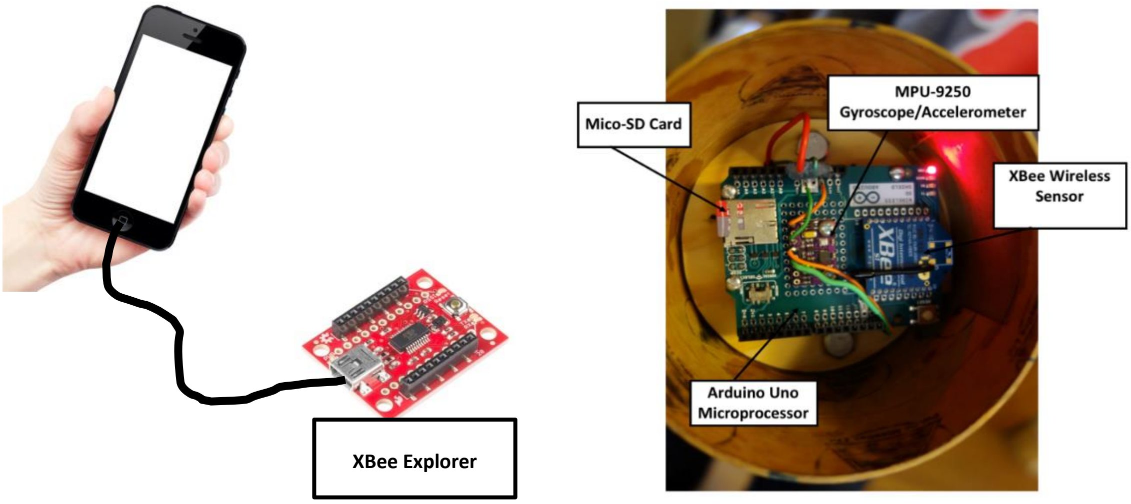

Figure 3-8. Wireless communication using XBee Explorer and XBee Series 1 Module in LEWIS2.

Figure 3-9. Recovery of the wireless sensor to analyze the data collected.

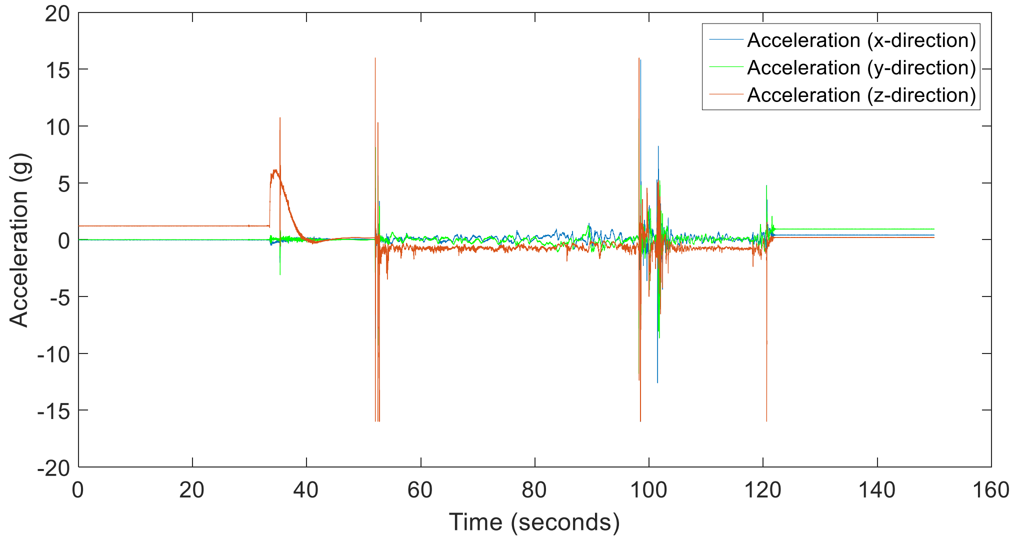

Figure 3-10. Acceleration of the Rocket.

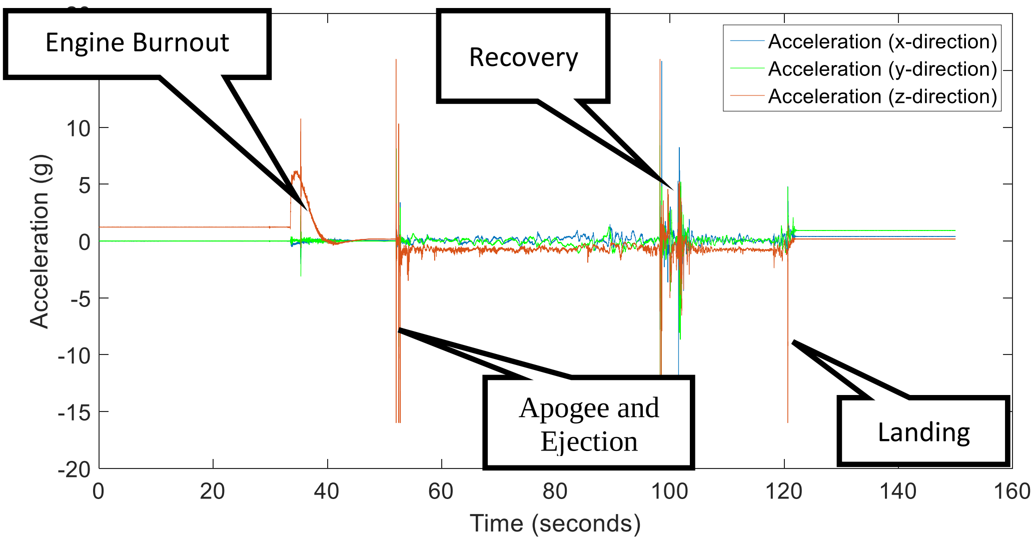

Figure 3-11. Angular velocity of the Rocket.

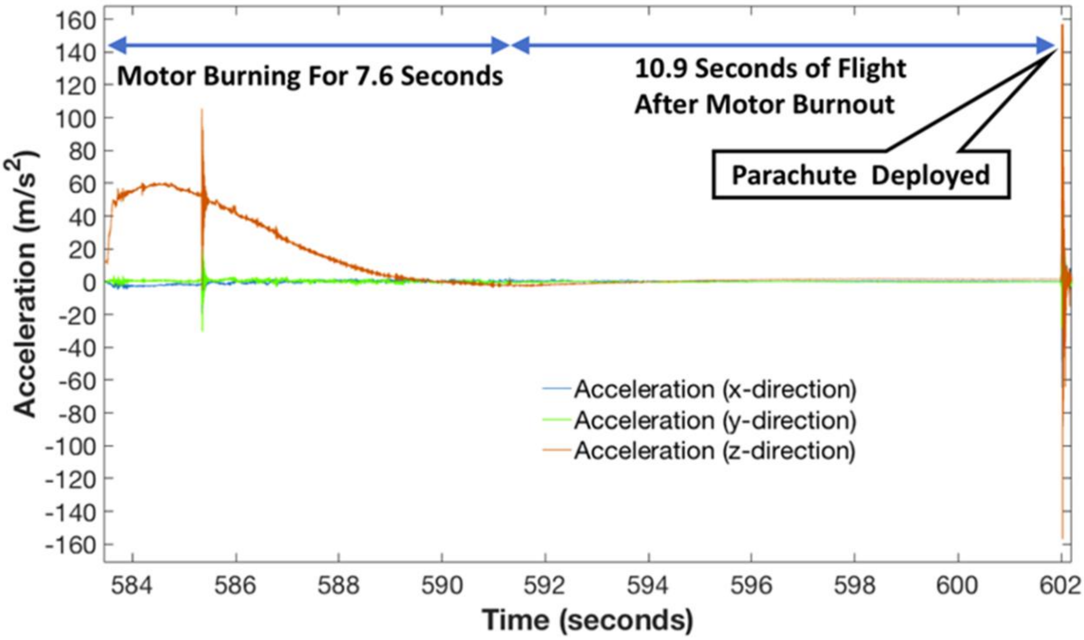

Figure 3-12. Initial events of the Rocket.

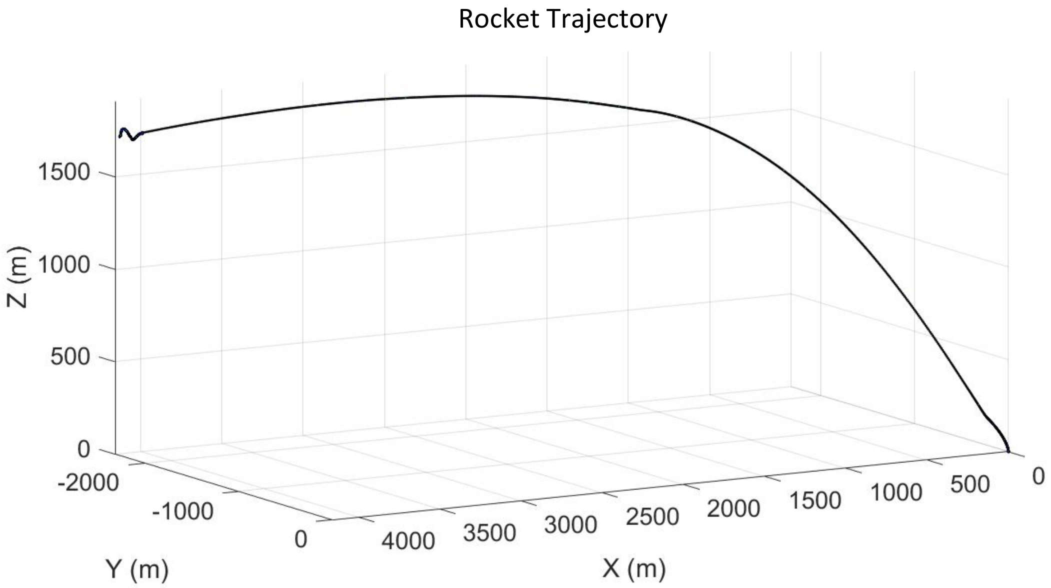

Figure 3-13. Rocket trajectory.

3.5. Ongoing development of LEWIS2

The effectiveness of LEWIS2 could be further enhanced through the use of a battery and solar panel component and a power boost component, as described below.

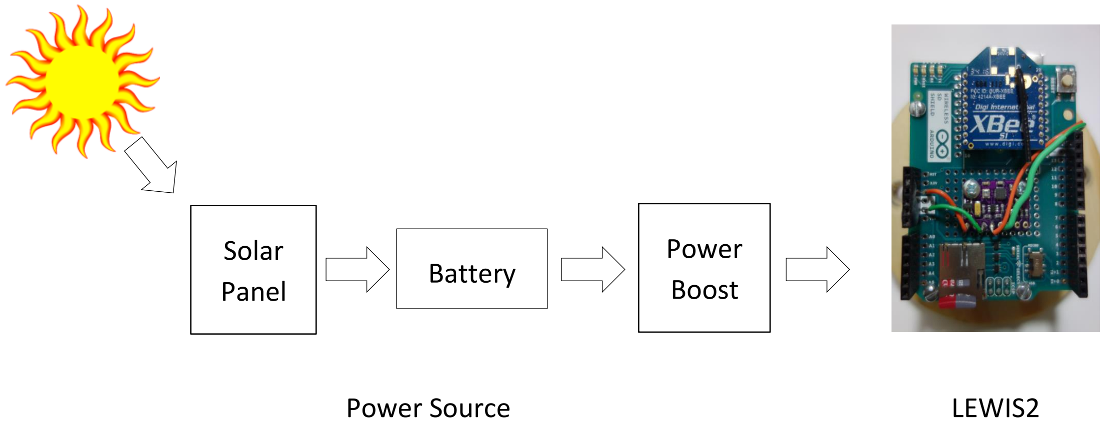

Figure 3-14. Potential development of LEWIS2.

The first innovation proposed for LEWIS2 development involves the integration of a lithium ion polymer battery and a solar panel used to charge the battery. Since LEWIS2 is applied outdoors in variable weather conditions and requires reliable power supply, the solar panel that is intended to charge the battery must be robust and efficient. For instance, a suitable option may be a Medium 6V 2W Solar panel manufactured by Voltaic Systems. As specified on the supplier's website (Voltaic, 2018), it is a reliable, waterproof panel, which is both UV and scratch resistant. It makes use of a highly efficient monocrystalline cell. The substrate of the panel is made of an aluminum/plastic composite, which is strong, resilient, and lightweight. The panel is designed for outdoor use, and it can be leaned on or dropped. It outputs 6V at 330 mA through a 3.5mm x 1.1mm DC jack connector.

This solar panel could be used to charge the lithium ion polymer battery, which in turn could be used to power the wireless sensor on LEWIS2. The output of such a battery ranges from 3.7V to 4.2V when it is fully charged, and it has a capacity of 2000mAh. While charging the lithium ion polymer battery, LEWIS2 will take the output from the solar panel, and it will feed it into a designated charging circuit. The role of this circuit is to control the potentially unstable output received from the solar panel and to ensure that the battery is steadily charged. It will also prevent the battery voltage from both overcharging and overusing, and it will protect against output shorts.

Another innovation that the author of this thesis proposes for the development of LEWIS2 is the application of a small-size power boost circuit, which converts the voltage of 3.7 volts supplied by the battery to 5 volts, which is the standard voltage applicable to microcontrollers and USB devices. As an example, a component that could be successfully applied is Adafruit Power Boost 1000C. As specified on the supplier's website (Adafruit, 2018), it is a small-size DC/DC boost converter module, which can be used with 1.8V batteries or higher. It converts the battery voltage to 5.2V DC, which makes it a suitable and safe circuit for all devices that use the voltage of 5V, including Arduino, Beagle Bone, and Raspberry Pi. The output voltage is slightly higher than 5V in order to compensate for the USB cable resistance. Power Boost 1000C is equipped with 4A DC/DC converter, which is powerful enough to produce 1A+ from the input that is as low as 2V, and a TPS61030 boost converter manufactured by Texas Instruments (TI). TPS61030 features a number of useful functions and devices, such as low battery detection and 4A internal switch, and it provides synchronous conversion, 700 KHz high-frequency operation, with excellent efficiency.

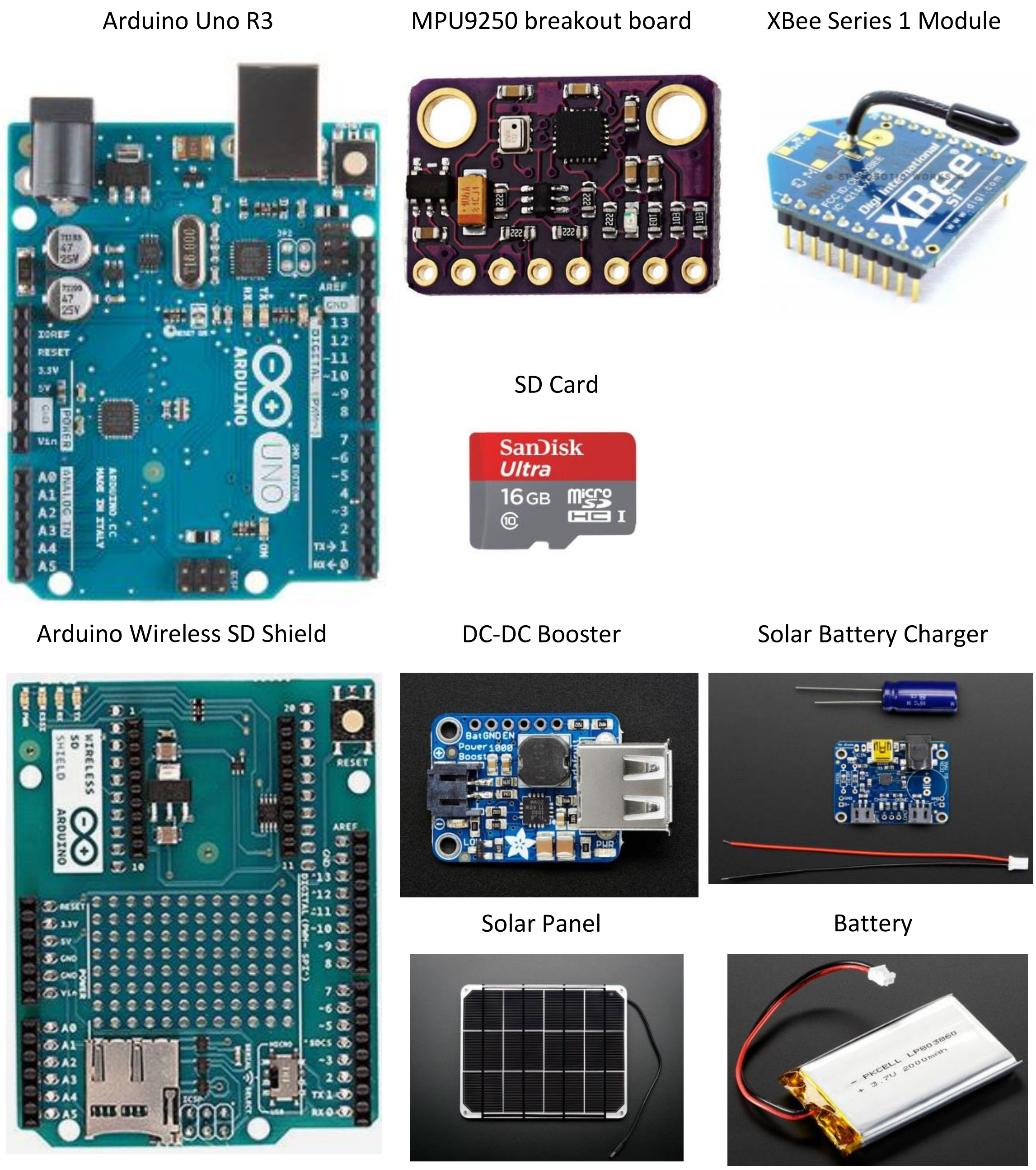

Figure 3-15. Components of the Arduino-based updated LEWIS2.

Figure 3-16. Other components updated LEWIS2.

Table 3-3. Main sensing platform components in the updated LEWIS2.

Element	Description	Market Price, $
Arduino Uno R3	Microcontroller	$4.00-$25.00
MPU9250	Sensor	$9.99
XBee Series 1 Module	Wireless transmission module	$25.00
Arduino Wireless SD Shield	Communication XBee S1 Module and Arduino Uno R3	$15.00
Solar Panel	Medium 6V 2W Solar panel - 2.0 Watt	$29.00
Solar Battery Chager	USB / DC / Solar Lithium Ion/Polymer charger - v2	$17.50
DC-DC Booster	Power Boost 1000 Basic - 5V USB Boost @ 1000mA	$14.95
Battery	Lithium Ion Battery - 3.7v 2000mAh	$12.50
SD Card	SanDisk Ultra 80MBs MicroSD Memory Card - 16GB	$10.00
Others:		
Box	Box plastic gry/clr 5.9"Lx5.91"W	$21.90
Magnet	CMS Magnetics Neodymium Round Base Magnet	$7.66
Switch	Heavy duty toggle switch 20/15A 125/277V, 2 HP	$7.81
USB Hub	Sabrent 4-Port USB 3.0 Hub	$15.99
USB Cable	USB2HAB2RA3 3 Feet USB Cable - M/M	$4.92
USB Mini Cable	USB Mini-B Cable - 6"	$1.95
	Total	**$198.17-$219.17**

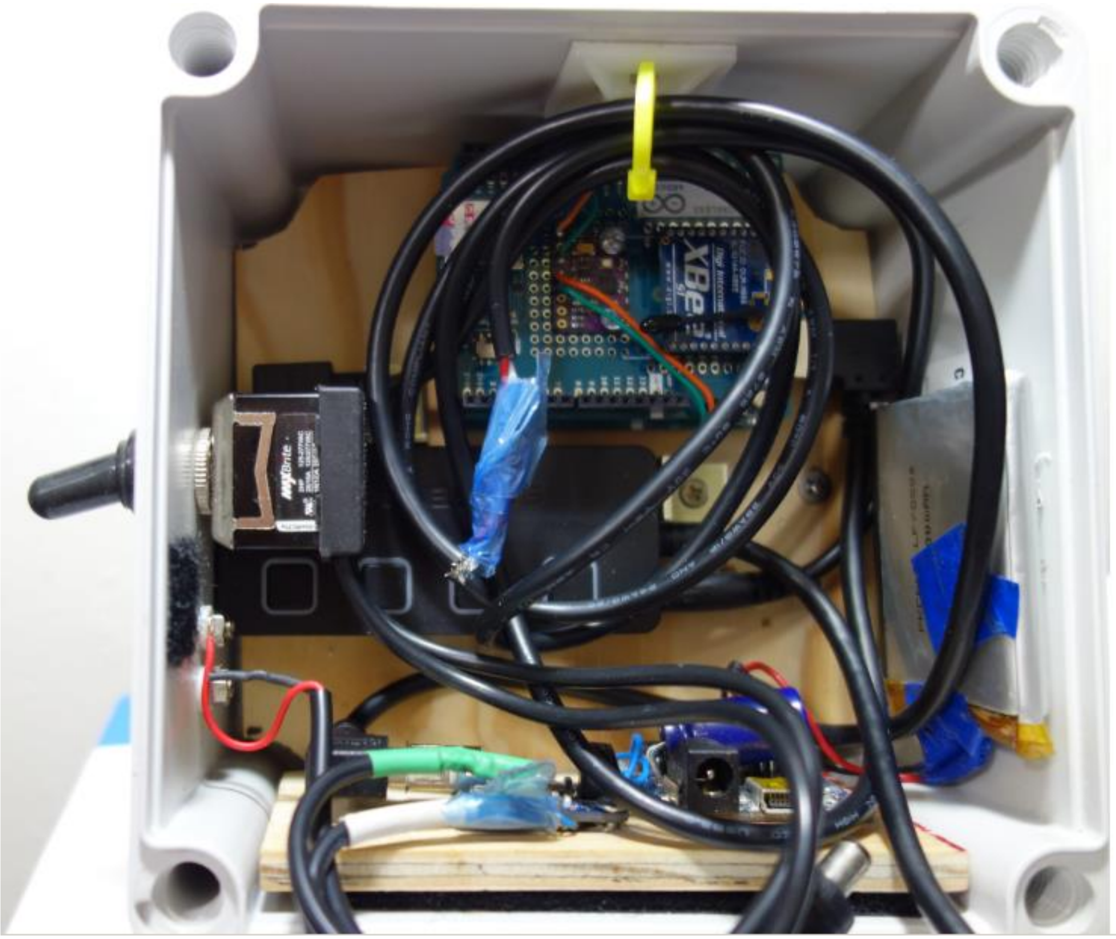

Figure 3-17. Assembled updated LEWIS2.

3.6. Future Work

Future tests will determine whether this sensor could work for several hours in difficult environments, as shown for the application in **Figure 3-23**.

Tramway Tower Measurements

The experiment took place in Sandia Peak Aerial Tramway, near Albuquerque, NM, US. The information concerning Sandia Peak Aerial Tramway provided below comes from the official website of the tramway http://www.sandiapeak.com/index.php%3Fpage=history-technology. The tramway was constructed in 1964-66 and entered service in on May 7, 1966. Since then, the original track cables became replaced in the spring of 1997. It is the longest aerial tramway in the USA, reaching 2.7 miles in diagonal length. In spite of the length, the tram cables receive support only from two towers located between the terminal buildings. Tower One is 232 feet tall, and it is situated at an elevation of 7,010 feet, whereas Tower Two is 80 feet tall and it is situated at an elevation of 8,750 feet. In order to evenly support the cables located between Tower Two and the lower terminal building, Tower One leans at an18 degree angle. Tower One is, in consequence, offset at more than 70 feet from the center of the tower base.

The tramcars pass at midway, at the point in which they are nearly 1,000 feet above the ground. The tram performs approximately 10,500 trips every year, and each tramcar has the loading capacity of 10,000 pounds up the mountain or 50 passengers, and its maximum rate is 200 passengers per hour.

For the purpose of the experiment, the author of this thesis and his colleagues from the University of New Mexico collected acceleration and angular velocity of the tramway's motion by placing the sensor LEWIS2 over the floor of the tramway's car. With the range for acceleration measurement being +/- 16 g's and for the angular velocity +/- 2000 degree per second for the LEWIS2 sensor, the sensor was able to record the full acceleration and angular velocity profile of the tramway's motion.

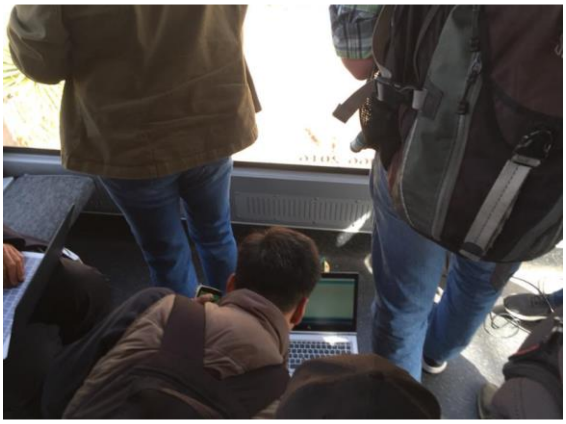

Figure 3-18. Placement and activation of the wireless sensor on the tramway.

Figure 3-19. Tramway.

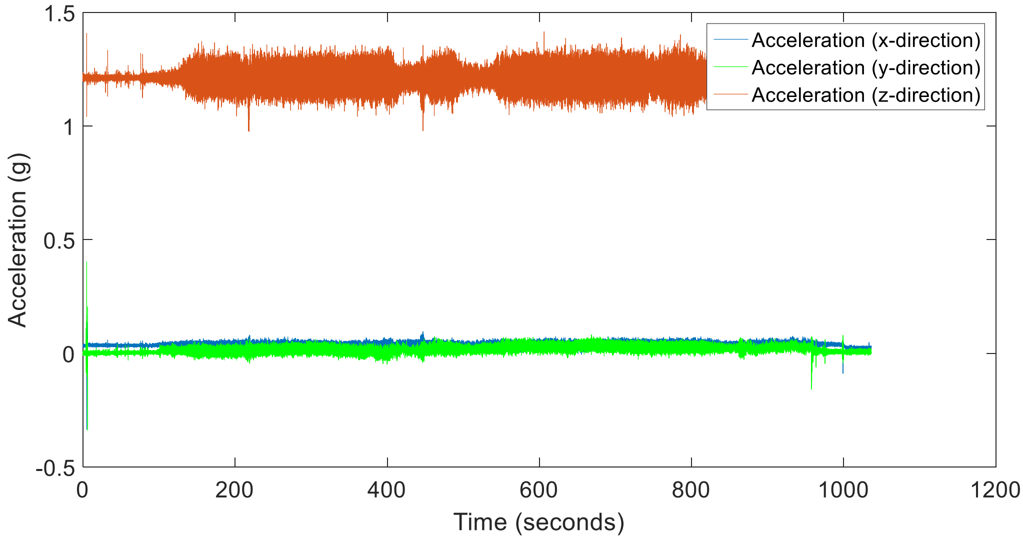

Figure 3-20. Acceleration during the tramway's travel.

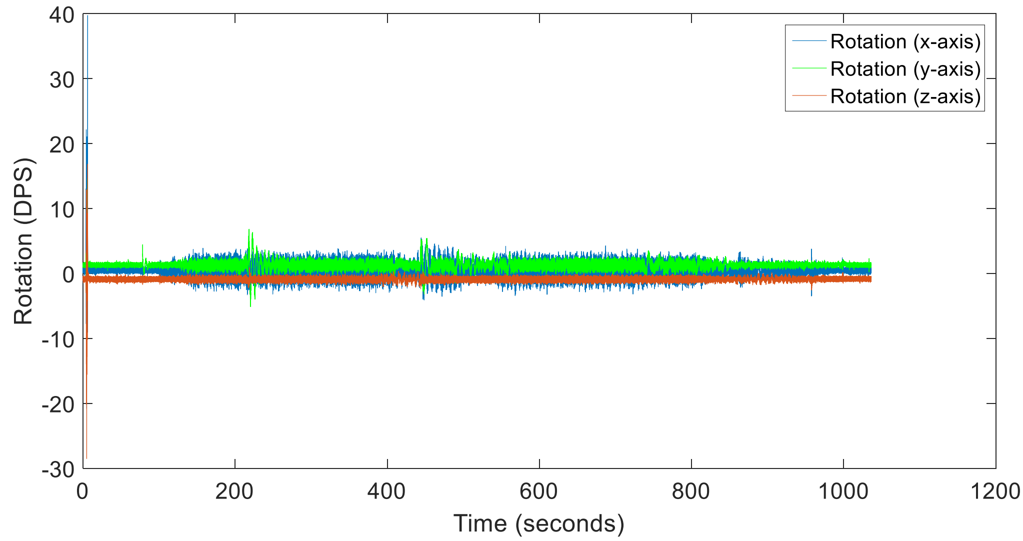

Figure 3-21. Angular velocity during the tramway's travel.

Figure 3-22. The updated LEWIS2 in Tramway Tower.

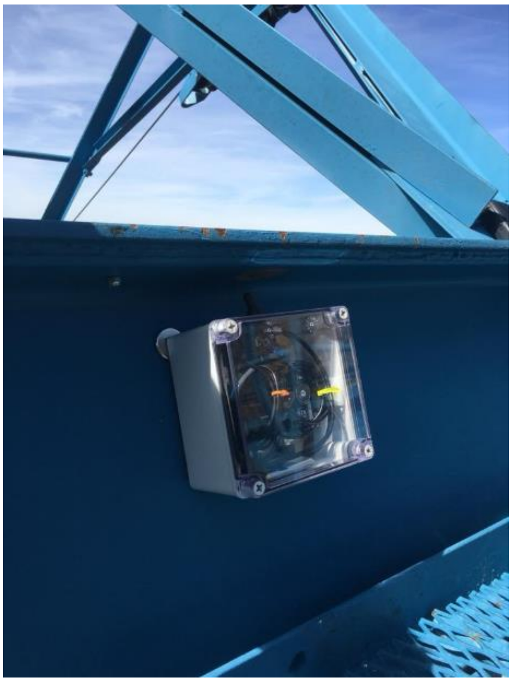

Figure 3-23. The updated LEWIS2.

3.7. Conclusions

This chapter has introduced a low-cost, battery-powered, low cost, efficient wireless intelligent sensor called LEWIS2. In comparison with its predecessor (LEWIS), it is equipped with an SD card and a Nanotech 1.0 Battery. The new LEWIS2 platform can collect data with low-cost sensor, MPU9250, measuring acceleration and angular velocity of different outdoor applications.

The author of this thesis has confirmed the efficiency of the LEWIS2 platform in a field experiment. The experiment involved using LEWIS2 with a rocket that was launched into the air. The purpose of using the rocket was to demonstrate LEWIS2 can work in environments with high vibration and displacements. This experiment also shows that LEWIS2 is capable of measuring acceleration and angular velocity to accurately estimate the trajectory of the rocket. More generally, it has been shown through this experiment that LEWIS2 can be successfully applied in new disciplines such as aerospace engineering, whereas the obtained results provide new information that can be used to optimize the design of rockets.

This chapter also provided recommendations concerning potential development that will further improve the characteristics of LEWIS2. The innovations include the use of an enclosure and a solar panel for outdoor applications. The enclosure will help protect LEWIS2 in variable weather conditions, whereas the robust solar panel will be used to charge the battery, providing a reliable power supply and thus improving the reliability of LEWIS2 in outdoor applications.

Future development of the sensor may include performing experiments to determine how the LEWIS2 sensor works in difficult environments for an extended period of time. The author of this thesis has already carried out a preliminary experiment of this type, which involved placing LEWIS2 in a tall tramway tower to test its performance and measure the tower vibrations. Future work may contribute then to the general aim of this research, which is to support the capabilities for multiple field environments and structural responses of diverse infrastructures with low-cost, battery-powered, efficient wireless intelligent sensors.

CHAPTER 4. LOW-COST, BATTERY-POWERED, EFFICIENT WIRELESS INTELLIGENT SENSOR (LEWIS2): MEASURING REFERENCE-FREE TOTAL DISPLACEMENTS

4.1. Introduction

As was pointed out in the previous chapters, the safety and reliability of some engineering constructions like large dams, tall towers, tunnels, and long-span cable-supported bridges is very important, as they are principal components of industrial and economic infrastructure. Important worldwide issues, such as long-term life quality, sustainable economic growth, and reliability of provided services are contingent on the quality of the civil infrastructure. Since the civil infrastructure strongly affects all areas of human life, it is necessary to develop complex engineering systems, and to appropriately maintain civil structures. These structures may be subject to unexpected disaster scenarios, severe environmental conditions. Moreover, they may experience harsh loading, and are also subject to the aging process. The lack of proper maintenance may give rise to severe economic losses as well as lead to the loss of human lives.

It is a vital necessity to survey and to monitor the health and structural integrity of such constructions and to develop methods that allow reliable detection and localization of the areas that may have potentially experienced loss. A system that provides this information is termed the Structural Health Monitoring (SHM) system (see chapter 1 for a detailed discussion). The SHM systems have recently become more reliable due to the rapid development of new technologies and innovations, which include microprocessors, sensors, and wireless networks (see Chen & Ni (2018b) for an extensive discussion). Wireless sensor network (WSN) enables reliable and efficient monitoring of bridges, buildings, bridges, dams, mines, wind turbines, oil rigs, pipe lines, and other important structures (see Doebling et al. (1996) and Sohn et al. (2004) for comprehensive overviews).

As was observed in chapter 2, the advanced WSN-based SHM systems have important advantages compared to the conventional wire-bases SHM applications. First, since wireless communication is highly economical, and provides considerable cost reductions when compared with traditional, inflexible communication systems that require the application of wires. Moreover, the deployment time for a WSN based system may involve a few day or even several hours, which is a significant reduction in comparison to a wired system, whose deployment may take several months or years (see Chintalapudi, K. et al., (2006)). Second, the cost efficiency of WSN-based SHM also translates into better quality of the assessment: it is possible to apply many inexpensive wireless sensor nodes, which in turn leads to a more accurate level of monitoring. Third, a SHM system that uses WSN can take advantage of the capacities of wireless sensor nodes and implement real-time, independent monitoring (see Frangopol & Messervey (2009), Ko & Ni (2005), and Chen & Ni (2018b) for an overview).

The upcoming part of this chapter first describes the freight railway network in the USA as an example of a large and important civil engineering structure that needs constant and reliable monitoring due to its significance for the US economy. Next, the subsequent sections show how the monitoring can be improved through an application of a WSN-based SHM system and demonstrates general advantages of such a system. The research presented in this chapter builds on the analysis described in Ozdagli et al. (2017), which was developed on the basis of the LEWIS sensor. The author of this thesis has updated the results obtained by Ozdagli et al. (2017) by using a low-cost, battery-powered, efficient wireless intelligent sensor (LEWIS2), which was overviewed in chapter 3. This sensor is more advanced and provides better results that the LEWIS sensor used by Ozdagli et al. (2017).

As reported in Ozdagli et al. (2017), the U.S. freight rail, makes heavy use of its transportation network, having at its disposal 225,000km (140,000 miles) of rail track and carrying approximately 40 t of freight per person every year (FRA, 2016). According to the estimates of the U.S. Department of Transportation, demand for freight transported via the railway network will significantly increase by tonnage, up to 90% by 2035 (IBISWorld, 2016). In order to meet the demand and improve the transportation capacities, 2015 saw the investment of nearly $30 billion, with the aim of the expansion and enhancement of the current railroad infrastructure in the seven Class I railroads (Surface Transportation Board, 2016). The railroad industry is a large engineering system, which comprises several subsystems of infrastructure, including more than 100,000 bridges, which form a high density network, with one bridge corresponding to every 2.25km (1.4 miles) of track (Moreu, Kim, & Spencer, 2017). Since many of these bridges are already 100 years old, they require regular maintenance, (AREMA, 2003). In addition, it has been estimated by RSAC (the Railroad Bridge Working Group of the Railroad Safety Advisory Committee) of the Federal Railroad Administration (FRA) that timber railroad bridges constitute 24% of the complete bridge length in the United States (FRA, 2008), and that many of them are past their service life (Wipf, Ritter, & Wood, 2000). In consequence, the modernization of the bridge network requires significant financial investment, which is equal to 3–5% of the total capital expenditures allocated to the modernization and development of the bridge infrastructure (AAR, 2013). However, since railroad funds and resources are limited, maintenance, repair, and replacement (MRR) must be cost-efficient in their maintenance of the aging bridge network (TRB, 2006). In consequence, in order to ensure operational safety, many makeshift solutions are applied, such as the introduction of weight restrictions and speed reductions on trains that cross railroad bridges (Cambridge Systematics, Inc, 2007); (Lai, 2008); (Chen & Duan, 2014). Given the challenges posed by the decaying bridge infrastructure, railroad managers need to assess and quantify the conditions of the bridge structures in a reliable way so as to be able to make informed MRR decisions (Moreu, et al., 2015). A major challenge for the reliability of their inspections is the currently assumed practice, which demands visual inspection of bridges in regular periods of time, rated under predetermined service load (Moreu & LaFave, 2012); (Moreu, Spencer, Foutch, & Scola, 2017).

As was pointed out above, MRR need to be cost efficient. Furthermore, they need to be based on reliable quantitative data so that it provides valid information about structural integrity and in consequence improves the safety of railroad bridge operations. In accordance with the recommendations of The American Railway Engineering and Maintenance-of-Way Association (AREMA) measurements for evaluation of existing bridges must be taken during service operation (AREMA, 2010). Specifically, AREMA recommends that vertical chord deflections of timber bridges under live loads should not be higher than L/250, where L is the span length (Chapter 7, Section 3.1.15 in AREMA (2010)). Another recommendation concerns vertical deflections of steel bridges, which should not exceed L/640 (Chapter 15, Section 7.3.3 in AREMA (2010)). AREMA does not assume a relationship between structural performance and global responses, including transversal and longitudinal displacements. However, for railroad managers it is crucial to collect railroad bridge displacements during train traffic, as it provides information concerning the safety of operations and objective performance. Therefore, railroad owners require means of objective measurements of bridge responses under trains that can be compared with some thresholds in order to perform informed safety decisions. Moreu et al. (2015) shows that it is possible to relate bridge displacements that are collected with LVDTs to service conditions of timber bridges. Still, even though in principle bridge displacement may be measured by means of LVDTs or other contact-type sensors, recording such responses remains a challenge because frequently a fixed reference frame is not available (Gavin, Rodrigo, & Kathryn, 1998).

The limitations of reference-based displacement transducers can be overcome by integrating new sensing technologies (reference-free and noncontact) into monitoring systems. For instance, Stiros and Psimoulis (2012) and Psimoulis and Stiros (2013) report applying a noncontact robotic total station (RTS) in order to measure railroad bridge displacement responses. Correspondingly, Nassif et al. (Nassif, Gindy, & Davis, 2005) show laser Doppler vibrometer (LDV) to be an effective tool in the noncontact quantification of bridge displacements. However, what remains a challenge is the fact that RTS and laser systems still must be provided with a reliable stationary reference, which is frequently not available for long-term monitoring. For this reason global positioning system (GPS) technology was examined as a potential alternative for long-term bridge-monitoring activities (Ashkenazi & Roberts, 1997); (Wong, Man, & Chan, Real-time kinematic spansthegap, 2001); (Wong K. Y., 2004); (Watson, Watson, & Coleman, 2007); (Meng, Dodson, & Roberts, 2007); (Yi, Li, & Gu, 2013). Since the global navigation satellite systems may experience technical deficiencies, which cause measurement errors, Nakamura (2000) and Moschas et al. (2013) fuesed GPS and RTS systems, with the aim of improved sensing accuracy. Other fusion methods involved the synthesis of GPS with accelerometer (Kogan, Kim, Bock, & Smyth, 2008); (Smyth & Wu, 2007); (Moschas & Stiros, 2011) and with inertial measurement unit (IMU) (Puente, Solla, González-Jorge, & Arias, 2015). However, these solutions must be frequently equipped with expensive instrumentation in order to reliable measurement. Furthermore, many of the reports presented in the literature limit themselves to the vision-based and optical displacement measurement systems for bridges, for instance target- and nontarget-based image-processing methods (Olaszek, 1999); (Lee & Shinozuka, 2006a; 2006b); (Ribeiro, Calçada, Ferreira, & Martins, 2014); (Fukuda, Feng, & Shinozuka, 2010); (Feng, Feng, Ozer, & Fukuda, 2015a); (Feng, Fukuda, Feng, & Mizuta, 2015b), laser-tracking technology (Wahbeh, Caffrey, & Masri, 2003), and light detection and ranging (LiDAR), so as to determine static-load testing deflections (Dai, et al., 2014). Correspondingly, Kim and Sohn (2017) present a conceptual dynamic measurement system developed on the basis of the Kalman filter, which fuses LiDAR with LDV. However, a substantial problem with the vision-based and optical measurement methods is that they require (1) expensive optical systems which provide high resolution, (2) sophisticated algorithms that could be applied to improve measurement precision, and (3) a fixed point on the site where the tripod and camera could be set.

Measurement techniques that rely on the indirect derivation of displacements from multiple reference-free contact-type sensor data are able to collect bridge responses under train-crossing events, which can be used for safety and the prioritization of maintenance. For instance, slope measurements obtained with tilt meters have been applied to determine vertical bridge deflections by using shape functions (Hou, Yang, & Huang, 2005) and a cubic spline technique (Sanli, Uzgider, Caglayan, Ozakgul, & Bien, 2000). Kim and Cho (2004) and

Chang and Kim (2012) applied fiber Bragg grating (FBG)-type strain sensors in order to determine displacements via shape functions and mode shapes. In addition, Helmi et al. (2015) designed a method that combines tilt meters and FBG strain gauges and enables long-term real-time monitoring of bridges. Park et al. (2014) developed a wireless displacement sensing system that is able to extract displacements from strain readings and acceleration. These methods, however, face important challenges. First, they do not estimate or measure transverse responses. Second, for accurate measurement they frequently require a thorough understanding of the structure and the precise locations where the sensors are mounted on the bridge. Significantly, Moreu et al. (2015) demonstrates that it is possible to estimate transverse displacement of timber railroad bridges under service loads from accelerations by using finite impulse response (FIR) filters. Moreu et al (2015) further observe that since the FIR filter may only extract dynamic components, the displacement reconstruction method gave rise to estimation errors, and when this method was applied, the pseudostatic displacements were not captured properly while.

As has been pointed out above, each of the presented approaches has its own limitations. First, some of these methods necessitate the application of complicated structural models or costly technological apparatus to render accurate measurement. Furthermore, because of computationally complex algorithms required in the estimation and measurement processes of bridge responses, most of these approaches cannot be applied in real-time monitoring. An automated bridge inventory management system may strongly benefit from the possibility of obtaining real-time bridge displacements. Moreover, access to real-time data may help the industry make informed and rapid decisions about the prioritization of MRR operations, and in consequence maximize efficiency and performance Railroad Bridge infrastructure systems and networks.

As an alternative, the author of this thesis proposes a method that provides reliable accurate and inexpensive measurements of displacement, which can especially be used for timber railroad bridges that are subject to pseudostatic deflections because of asymmetric boundary conditions. This method makes use of measured real-time acceleration and rotation data that is captured with low-cost, reference-free, battery-powered efficient WS sensors (LEWIS2). The workings of the new method were tested and evaluated by the author of this thesis, analyzed the results of an experiment developing a timber pile bent model, in which the cap was attached to a shake table, whereas the ground level was attached to a rigid frame. In the experiment setup reported here, the shake table excited a representative pile with realistic traffic conditions that correspond to two different speeds (Track Class 1 and 2) regulated on timber railroad bridges in North America, while transverse accelerations and rotations captured with relevant sensors were converted to displacements in real time by applying the proposed method. The simplified model of the timber railroad bridge was capable of capturing the basic performance of timber trestles under trains. The transverse displacements obtained in the experiment were compared to the responses that were estimated via the proposed method. The main conclusion of this experiment was that it is possible to obtain transverse displacements of bridges through the application of reference-free measurements. More generally, this experiment also showed that bridge responses can be measured quickly, conveniently, and reliably without the necessity of having a fixed reference in real time, and that it also improves the accuracy of informed decisions in MRR operations.

4.2. Reference-Free Total Displacements

This section introduces the principles of estimating reference-free total displacements from acceleration measurement.

Principles of Total Displacement Estimation

The procedure for estimating total displacement is divided into the following three stages: (1) data collection, (2) data filtering, and (3) data fusion. The first stage, is devoted to obtaining acceleration and inclination data via accelerometers. The second stage focuses on measurement filtering and it leads to the extraction of the pseudo-static and dynamic components. In the third stage, extracted records are fused in order to obtain the total displacements. Eq. (1) will define the complete transverse displacements, Δ_t:

$$\Delta_t = \Delta_d + \Delta_p \tag{1}$$

where Δ_d and Δ_p represent the dynamic and pseudostatic components of the total transverse displacements, respectively. The subsequent sections describe how these components can be obtained.

4.2.1. Dynamic Displacement Estimation

To extract the dynamic displacement from acceleration measurement, a finite impulse response (FIR) filter is used (Lee, Hong, & Park, 2010).

$$\Delta_d = \left(L^T L + \lambda^2 I\right)^{-1} L^T L_a \bar{a}(\Delta t)^2 = C\bar{a}(\Delta t)^2 \tag{2}$$

$$\lambda = 46.81N^{-1.95} \tag{3}$$

Moreu et al. (2015), Ozdagli et al. (2017; 2018) and Park et al. (2014; 2016), provided a demonstration of the FIR filter in the dynamic displacement estimation.

4.2.2. Principles of Inclination Sensing and Pseudostatic Displacement Extraction

Inclination sensing makes use of gravity and its projection on the axes of the accelerometers. This approach draws significant benefits from DC-type accelerometers, which are capable of measuring static gravity vectors. For instance, the capacitive MEMS-type accelerometer is able to provide precise 1-g response under gravitational acceleration. Fig. 6 illustrates an accelerometer measuring the acceleration in its x-axis. As soon as the accelerometer tilts, the projection of the gravitational acceleration, g on the x-axis of the sensor, produces an output acceleration Ax, which is equal to the sine of the angle θ between the accelerometer x-axis and the horizon axis, which is orthogonal to the gravity vector. The resulting acceleration and angle can be formulated in the following way:

$$A_x = g \times \sin(\theta) \tag{4}$$

$$\theta = \sin^{-1}(\frac{A_x}{g}) \tag{5}$$

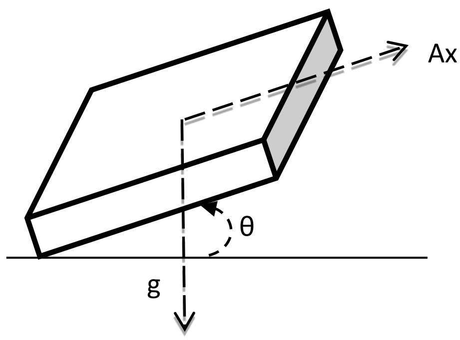

Figure 4-1. Sensing rotation using a single-axis accelerometer.

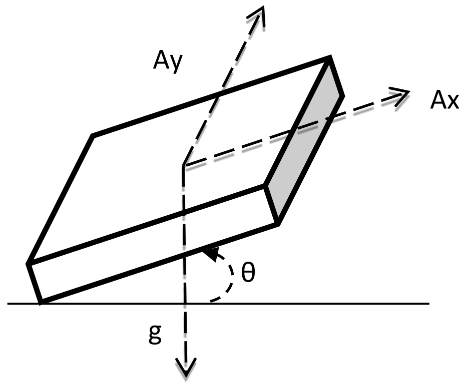

Figure 4-2. Sensing rotation using two axes.

Single-axis inclination sensing may give imprecise readings when the resolution of the sensor is too low. The minimum required resolution is determined in the following way:

$$R = g \times (\sin(N + P) - \sin(N)) \tag{6}$$

where N is the range of angle to measure; and P is the minimum angle to measure (Fisher, 2010). In order to improve the accuracy, LEWIS2 in addition measures the projection of the gravity vector onto the y-axis (Fig. 7). In order to convert the measured acceleration in the y-axis A_y to the inclination angle, the cosine of the angle θ between the y-axis and the gravity vector is calculated, as follows:

$$A_y = g \times \cos(\theta) \tag{7}$$

$$\theta = \cos^{-1}(\frac{A_y}{g}) \tag{8}$$

By combining Eqs. (4) and (7), it is possible to compute the ratio between A_x and A_y and establish the tangent of the inclination angle

$$\frac{A_x}{A_y} = \frac{g \times \sin(\theta)}{g \times \cos(\theta)} = \tan(\theta) \tag{9}$$

Applying the inverse tangent function on both sides of Eq. (8) gives the direct inclination.

$$\theta = \tan^{-1}\left(\frac{A_x}{A_y}\right) \tag{10}$$

This approach is well documented and used in many applications, including mobile phone orientation and virtual reality headsets (Fisher, 2010).

4.2.3 Pseudostatic Displacement Estimation from Rotation Data

The FIR filter applied for computing zero-mean displacement cannot capture low-frequency pseudostatic characteristics of the displacements. In order to accurately measure the total displacement, the method developed in this chapter reconstructs the pseudostatic component by calculating the inclination.

Deep pile foundations of the timber bents resist lateral loads because of soil resistance. Due to complex soil conditions, it is rather difficult to model the boundary conditions of embedded piles. However, in order to account for the soil resistance and the enhance the reliability of the improve, the pile can be idealized as equivalent to a free-standing cantilever column, which is commonly acknowledged in the rail-road bridge industry as being representative of timber railroad bridge design and performance (Davisson, 1970). In this study we model a timber railroad pile bent as a cantilever column considering soil–structure interaction. A detailed analysis of cantilever simplification is provided in Ozdagli et al. (2017).

Assuming lateral load, P which produces pseudostatic displacement Δ_p, the resulting pseudostatic rotation will be equal to θ_p. In accordance with Euler–Bernoulli beam theory:

$$\Delta_p = \frac{PL^3}{3EI} \tag{11}$$

$$\theta_p = -\frac{PL^2}{2EI} \tag{12}$$

where L is the length of the cantilever column; E is Young's modulus; and I is moment of inertia of the column section.

The combination of Eqs. (11) and (12) results in the ratio between Δ_p and θ_p, which does not include material and section geometry properties

$$\frac{\Delta_p}{\theta_p} = -\frac{2}{3}L \tag{13}$$

By rewriting Eq. (13) as a function of θ_p, pseudostatic displacement yields the following:

$$\Delta_p = -\frac{2}{3}\theta_p L \tag{14}$$

This chapter provides a validation for the estimation of pseudostatic displacement observed because of asymmetric loading. Other potential contributions to pseudostatic displacement components, including shear, local effects, or other nonlinear behaviors are not addressed in this study.

For typical bridge measurements, accelerations A_x and A_y applied in the calculation of the angle contain both high-frequency and low frequency responses. Thus, inclination angle may not settle to a pseudostatic value during a train crossing. In consequence, the estimated inclination still contains both dynamic and pseudostatic components. To attenuate the dynamic components and extract low frequency components, a moving average (MA) filter is applied. The resulting filtered data can be rendered in the following way

$$\theta_p[i] = \frac{1}{n}\sum_{j=0}^{n-1} \theta_t[i+j] \tag{15}$$

where θ_t is total rotation containing both dynamic and pseudostatic components; i is ith time step; and n is number of points in the average, that is the size of the averaging window.

The size of the averaging window is adjusted on the basis of the frequency content of the total displacement. For instance, a train crossing a bridge at a faster speed may trigger higher frequency displacements (Moreu, et al., 2014). In such scenarios, increasing n will be more effective in removing dynamic content from the input signal. As soon as the pseudostatic inclination is extracted, Eq. (15) can be applied to calculate the pseudostatic displacements.

4.3. Experimental Validation

This section provides an explanation of the experimental setup that was applied in order to validate the proposed method. The first part overviews the simplified cantilever beam model selected for the experiment. The subsequent part addresses the sensor placement and the instrumentation necessary for the method. Finally, this section provides an analysis and evaluation of transverse displacements, accelerations, and rotations collected from the experiments in order to assess the performance of the developed method.

Experiment

As shown in **Figure 4-3** and **Figure 4-4**, this study uses a cantilever column simulating the dynamic behavior of a timber railroad bridge pile (b). The pile model is inverted in such a way so that the free end of the cantilever (f) is excited by a shake table (i) capable of reproducing the bridge deck response to train crossings (**Figure 4-3** and **Figure 4-4**). To move the pile tip freely, it is placed between two L-brackets (h). The pile free end is restricted by sponge damping pads (g) attached to L-brackets acting as equivalent rollers to damp out excessive vibration while preserving the cantilever behavior action. Correspondingly, the fixed end of the pile (a) is secured to a rigid frame (e) that represents the stiff ground condition. c) LVDT

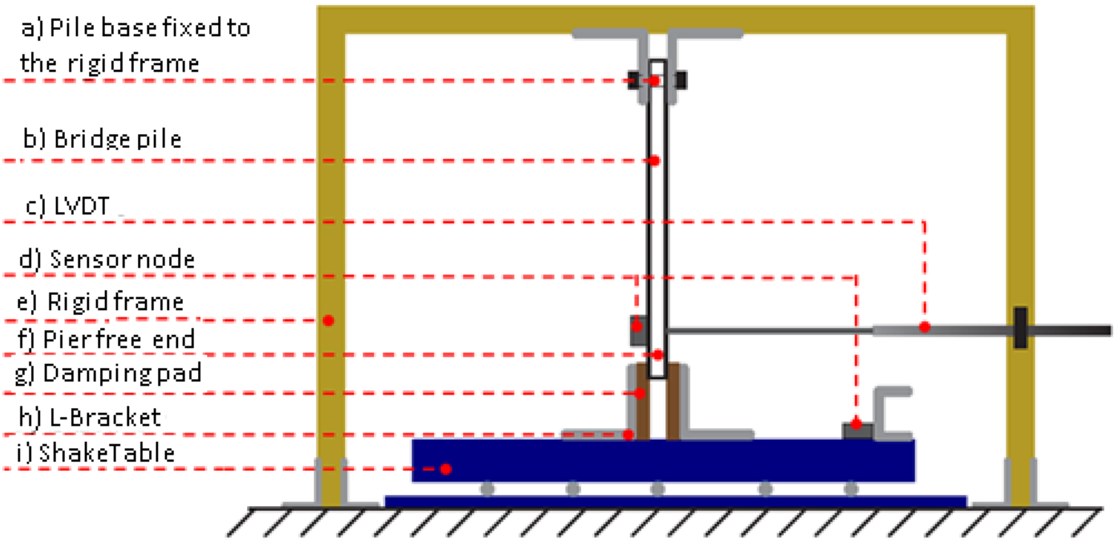

Figure 4-3. Instrumentation layout.

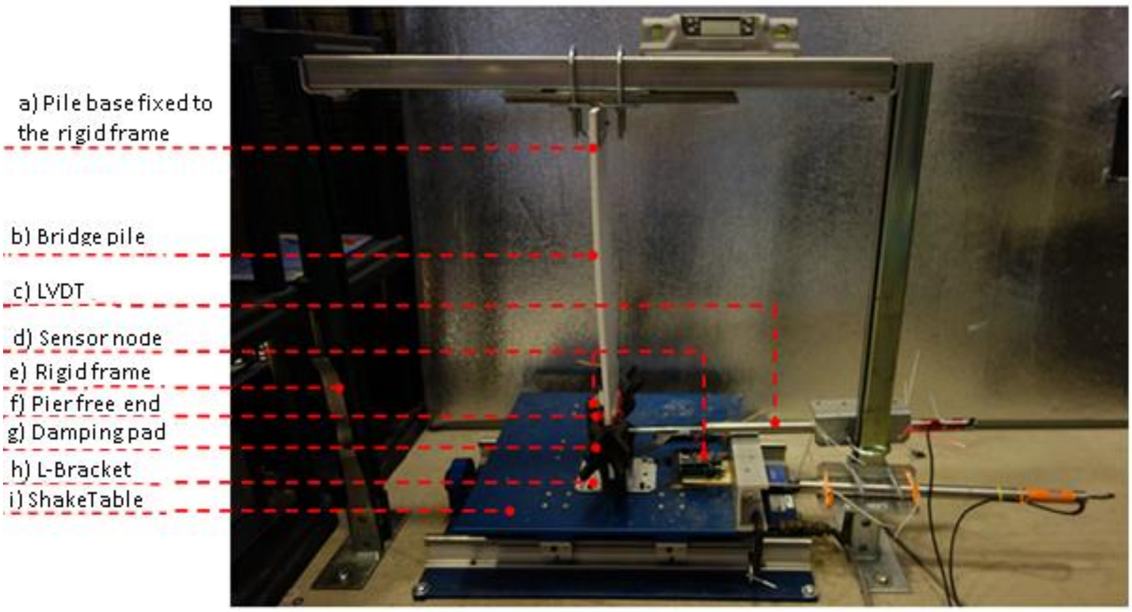

Figure 4-4. Experiment.

Instrumentation

A Quanser Shake Table II (as it is shown in **Figure 4-4**) with a maximum stroke of $\pm$76 mm ($\pm$3 in) drives the column. A low-cost, battery-powered efficient WS (LEWIS2) (d) is placed on the column. The accelerations measured by this sensor are applied to compute the pile rotation and extract the pseudostatic displacements, as explained in previous sections. The sensor measures both vertical and horizontal responses with respect to gravitational accelerations. The sensor selected for this experiment can deliver true DC response and measure gravity and other types of sustained accelerations. Another LEWIS2 (d) is attached to a C-bracket on the shake table. A linear variable differential transducer LVDT (c) is placed to register the displacement of the pile at the point where the accelerometer pair is located.

The total displacement responses of the Bluford Bridge, a timber bridge located near Edgewood, Illinois, Chicago, USA, have been recorded by Moreu et al. (2015). These bridge displacement records are applied as the input to the shake table so as to excite the pile model. **Table 4-1** provides a description of the 5 train velocities. The train speeds discussed herein are typical of and realistic for freight traffic in U.S. operations.

Table 4-1. Train Crossing Details.

Train number	Velocity km/h (mph)
1	24.9 (15.5)
2	33.9 (21.0)
3	31.1 (19.3)
4	41.5 (25.8)
5	41.0 (25.5)

Performance Evaluation Indices

The performance indices are prepared in such a way so that smaller values indicate better performance.

$$E_1 = \frac{|\Delta_{est}|_{max} - |\Delta_{meas}|_{max}}{|\Delta_{meas}|_{max}} \tag{16}$$

$$E_2 = \frac{RMS(\Delta_{est} - \Delta_{meas})}{RMS(\Delta_{meas})} \tag{17}$$

4.4. Results and Evaluation

This section provides the outcomes of the experiment. As has been illustrated in the previous part of the thesis, the five bridge displacement profiles of different types captured on the field were input to the shake table. The shake table excited the commercial LVDT and the proposed LEWIS2. The LEWIS2 performs the following two actions: it first collects the acceleration and angular velocity in the three axes at a sampling rate of fLS = 500 Hz, and subsequently it transmits the captured data to base stations. We used the VibPilot to record the responses produced by the LVDT, at a sampling rate of fVP = 1024 Hz. Next, for comparative purposes and verification, we resampled the data that had been collected by LEWIS2 at fLS, 1024 Hz. Subsequently, we converted the measurement of acceleration previously collected by the LEWIS2 sensing platform to displacement, in the offline mode. In the last stage, the displacement data that had been derived from the LEWIS2 platform was compared with the reference signal that had been collected with the LVDT.

As shown in **Figure 4-5** to **Figure 4-9**, the dynamic displacement obtained with LEWIS2 is quite different than the reference displacement obtained with the LVDT.

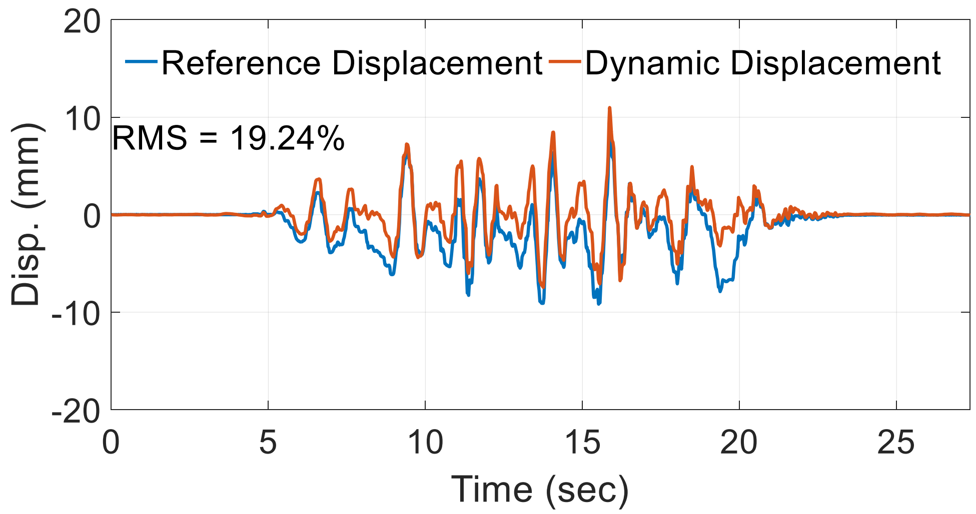

Figure 4-5. Reference and dynamic displacement – Train 1.

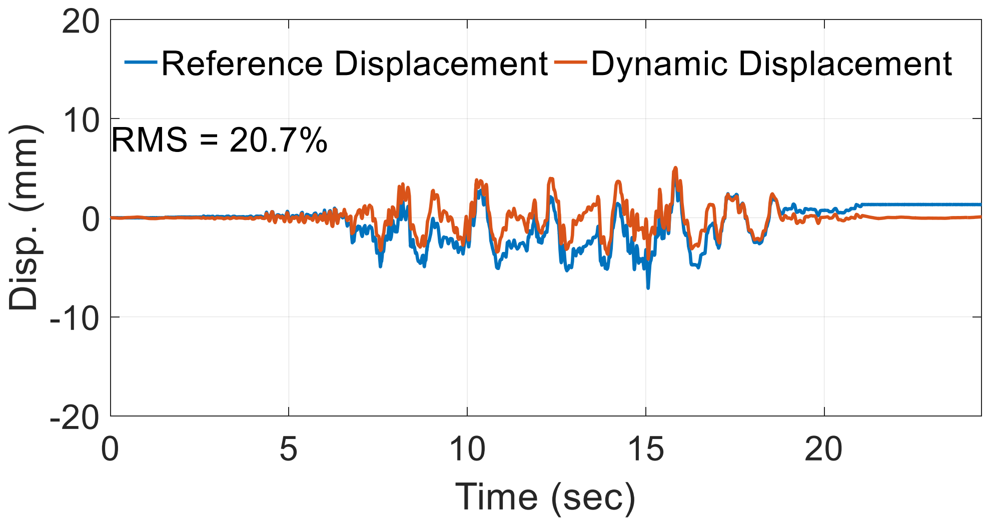

Figure 4-6. Reference and dynamic displacement – Train 2.

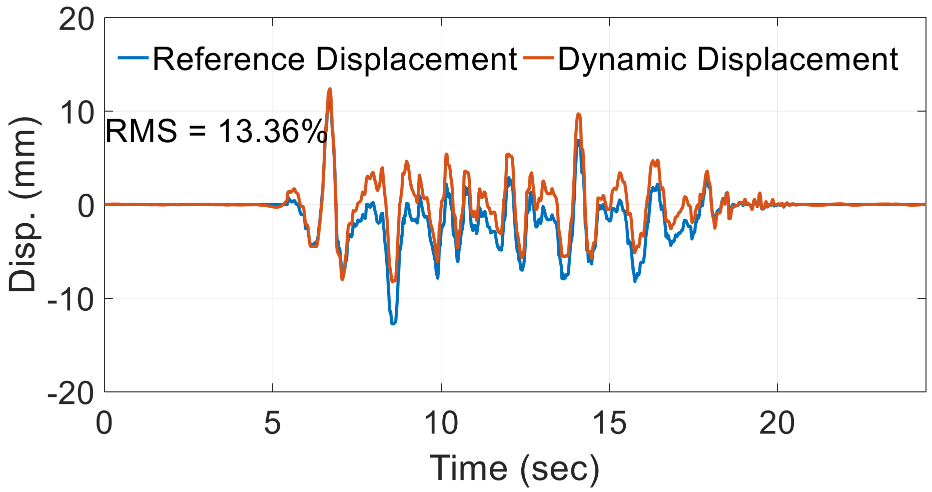

Figure 4-7. Reference and dynamic displacement – Train 3.

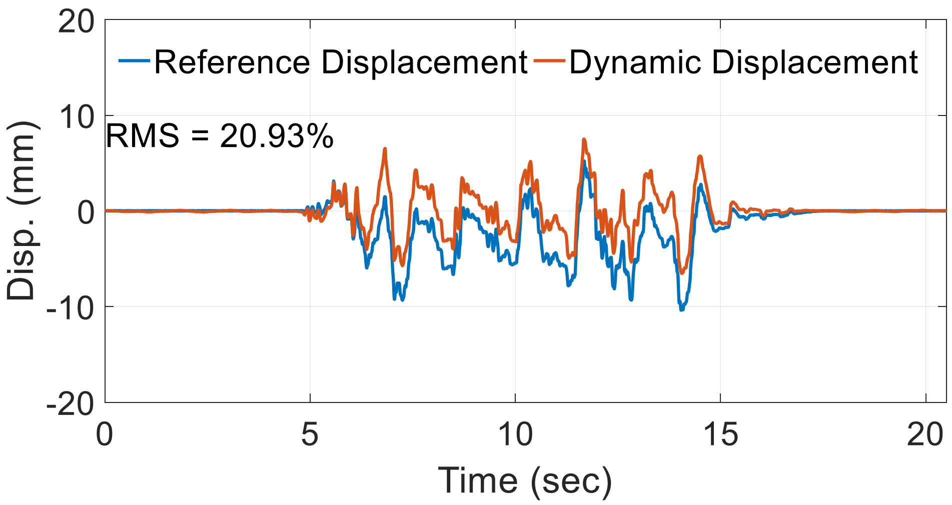

Figure 4-8. Reference and dynamic displacement – Train 4.

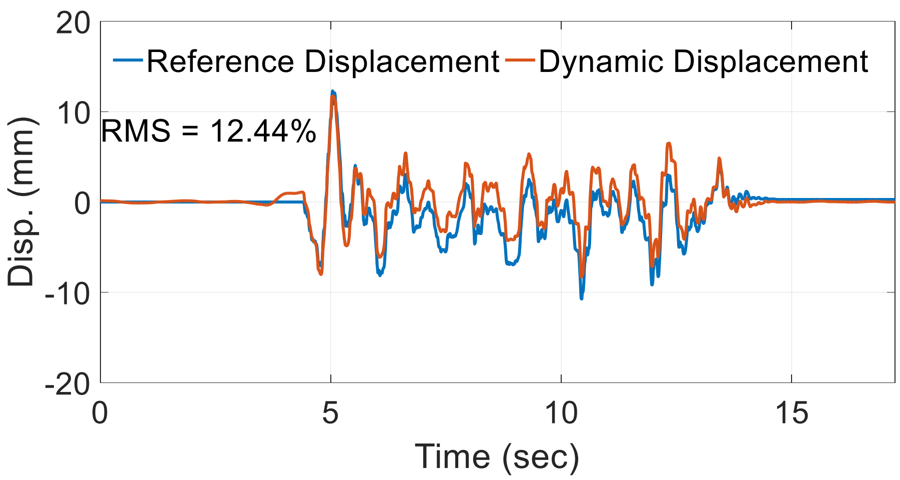

Figure 4-9. Reference and dynamic displacement – Train 5.

We obtained Root Mean Square (RMS) errors, which are presented in Table 4-1.

Table 4-1. RMS Dynamic Displacement.

Train number	RMS (%)
1	19.24
2	20.70
3	13.36
4	20.93
5	12.44

To obtain the total displacement, we calculated the pseudostatic displacement with the procedure described in 4.2 and obtained the displacements showed in **Figure 4-10** to **Figure 4-14**.

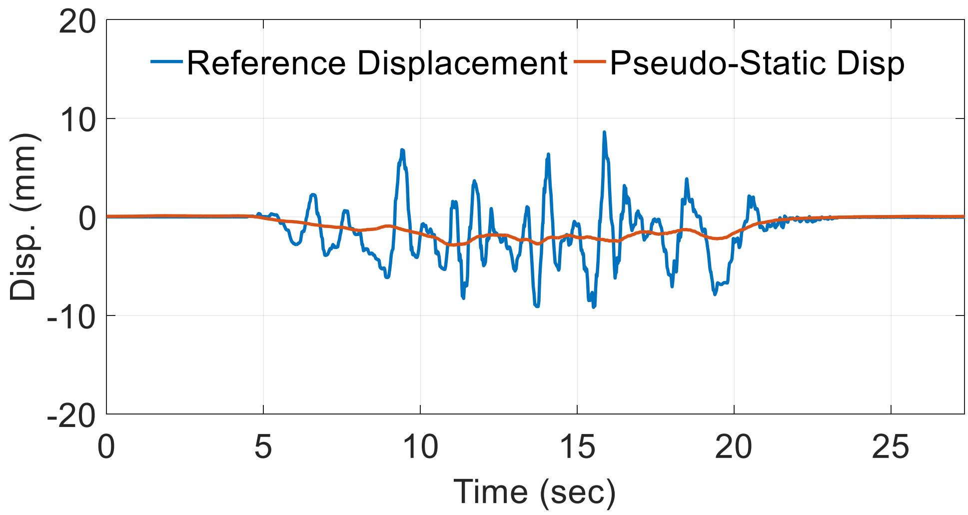

Figure 4-10. Reference and pseudo-static displacement – Train 1.

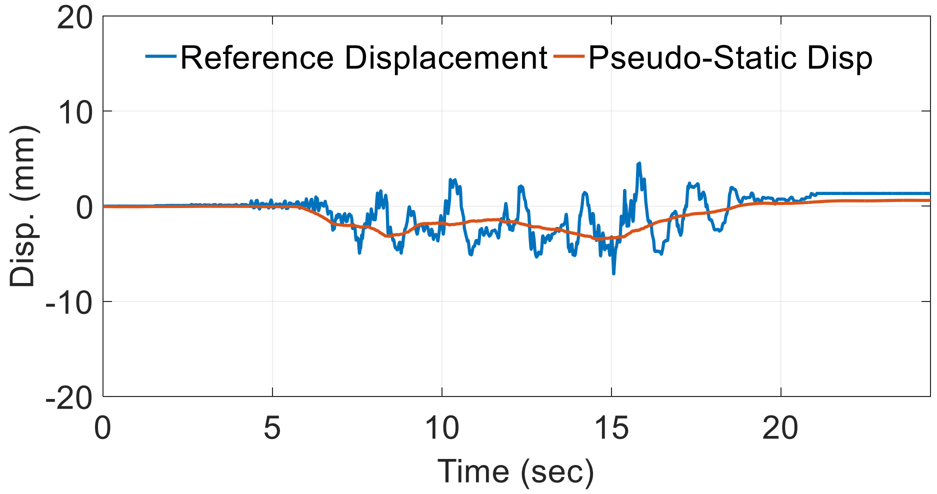

Figure 4-11. Reference and pseudo-static displacement – Train 2.

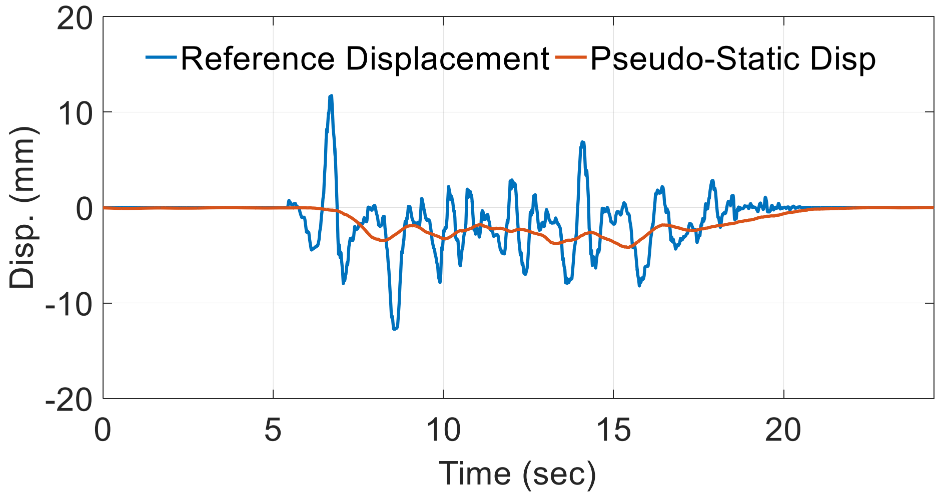

Figure 4-12. Reference and pseudo-static displacement – Train 3.

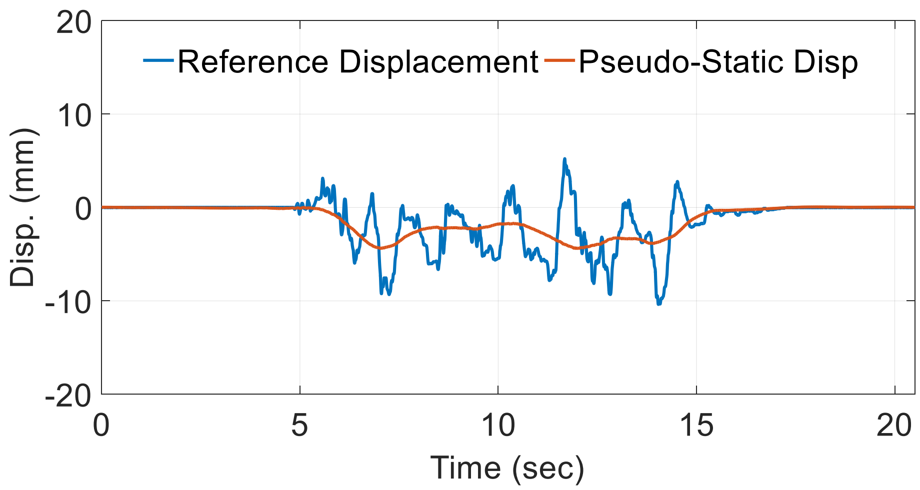

Figure 4-13. Reference and pseudo-static displacement – Train 4.

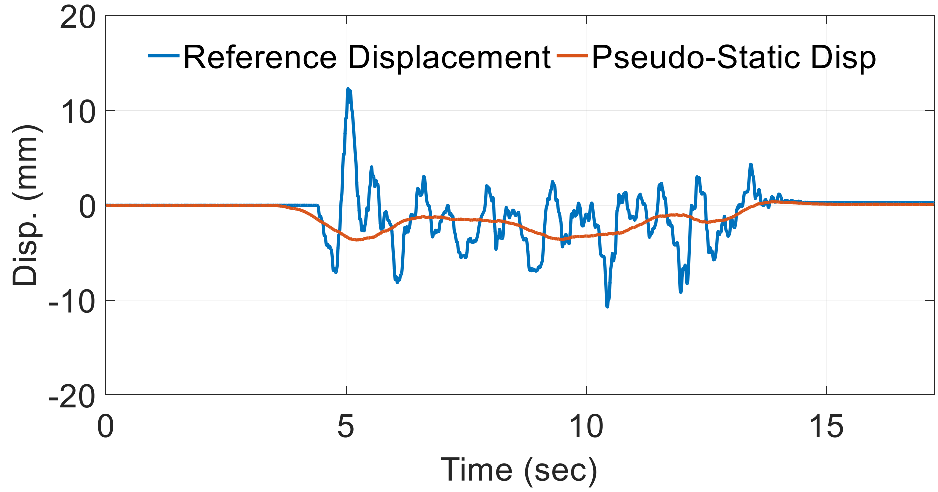

Figure 4-14. Reference and pseudo-static displacement – Train 5.

The sum of dynamic displacement and pseudostatic displacement gives us the total displacement shown in **Figure 4-15** to **Figure 4-19**.

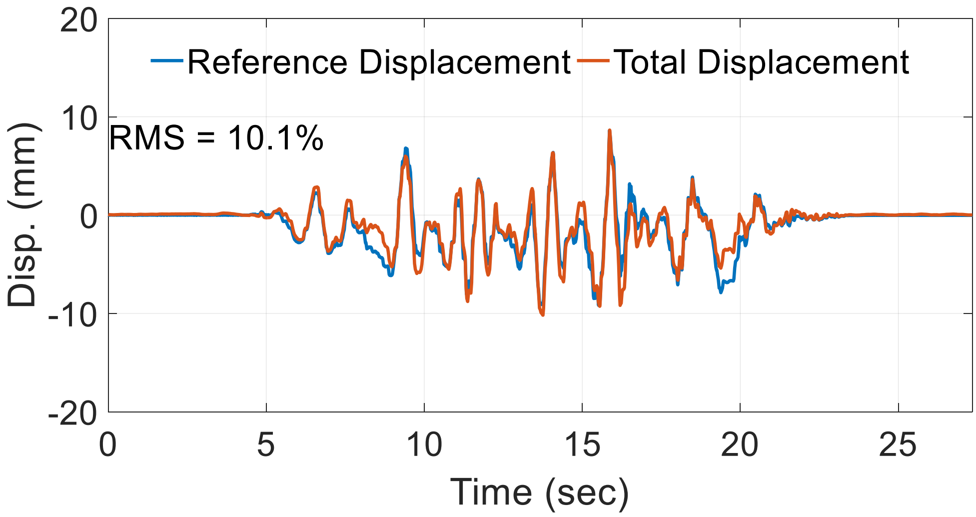

Figure 4-15. Reference and total displacement – Train 1.

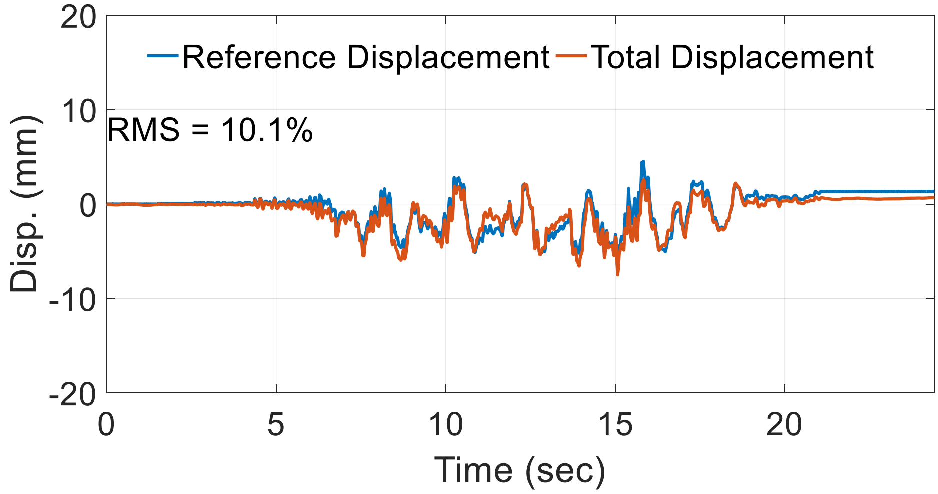

Figure 4-16. Reference and total displacement – Train 2.

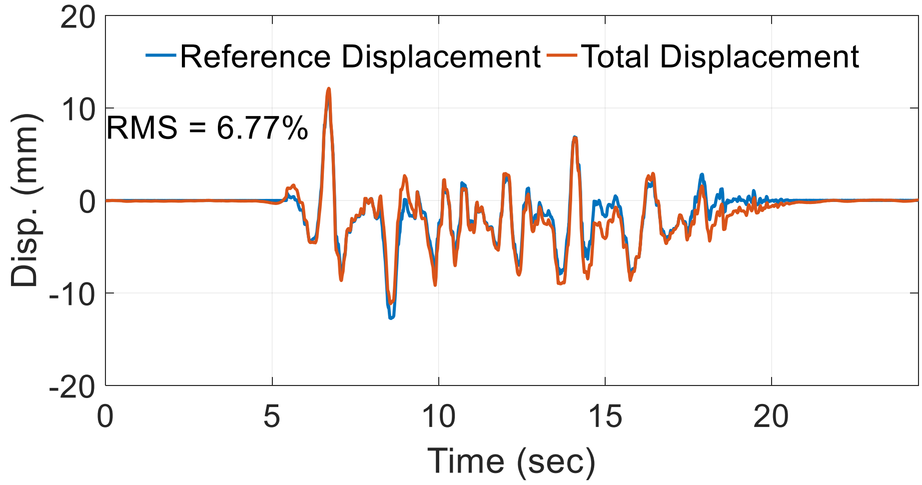

Figure 4-17. Reference and total displacement – Train 3.

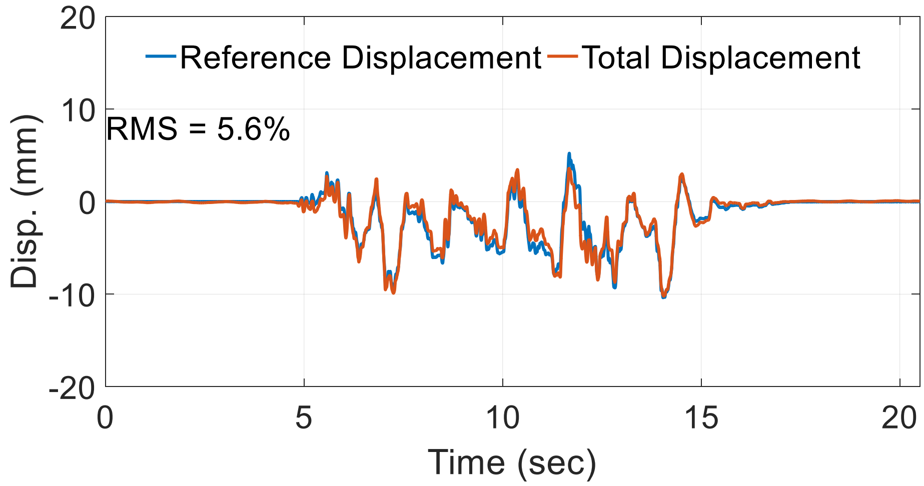

Figure 4-18. Reference and total displacement – Train 4.

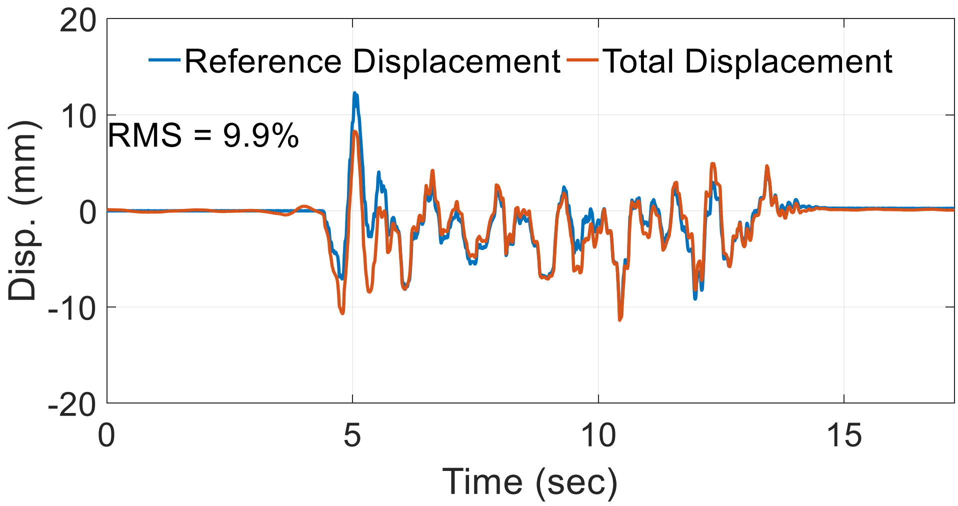

Figure 4-19. Reference and total displacement – Train 5.

In order to evaluate the correctness, accuracy, and the effectiveness of the LEWIS2 platform in quantitative terms, we computed the performance indices that were proposed in the previous part of this thesis. They are presented in **Table 4.2** and in **Figure 4-20**, which shows the errors E1 and E2 indices in percentage terms for all the events of train crossings.

Table 4-2. Performance Results.

Train number	$E_1(\%)$	$E_2(\%)$
1	10.94	10.11
2	5.35	10.10
3	4.91	6.77
4	1.60	5.60
5	7.45	9.90

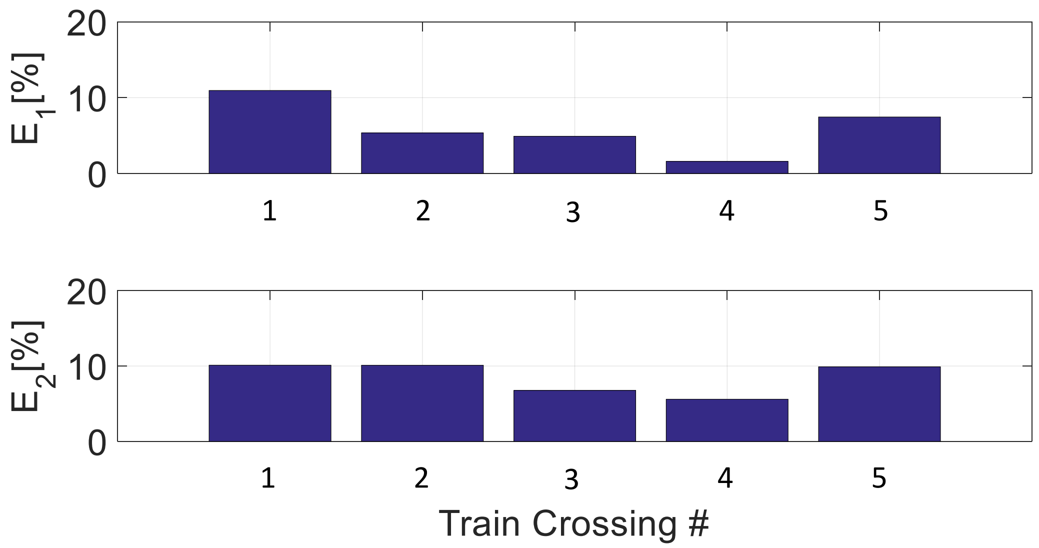

Figure 4-20. Performance evaluation results for total displacement estimation.

As the results presented in **Table 4.2** and in **Figure 4.20** show, the LEWIS2 estimates bridge displacements accurately. The highest value of E1 corresponding to the largest displacement error consolidates to 11%. Three out of the five train crossings produce less than 5.5% of errors in the LEWIS2 platform. The peak errors are attested for the crossings of Trains 1 and 5, and are 11% and 8%, respectively. The RMS (E2) errors have a range between 5 and 11%, whereas the peak RMS (E2) error is 11%, attested for Train 1 in the LEWIS2 platform.

Importantly, the discrepancies in the measurements of displacement can be removed by the FIR filter. Thus, the responses in the time domain produced by the LEWIS2 sensor are comparatively similar to the signal that was received from the reference LVDTs.

To summarize, the results of the experiment presented in this section demonstrate that the LEWIS2 is capable of giving accurate estimates of the dynamic transverse displacement for railroad bridges. The LEWIS2 sensing platform is very economical and does not need to be fixed to a reference frame. Furthermore, it gives comparable performance results to those produced by the commercial LVDT.

4.5. Conclusions

The chapter has addressed a new method to estimate transverse bridge displacements by aggregating data obtained from multiple reference-free sensors by minimally relying on the structural properties. This method was originally developed by Ozdagli et al. (2017) using commercial accelerometers. In this chapter the displacements were calculate via the new LEWIS2 sensing platform.

A FIR filter is used to extract dynamic displacement from acceleration. Likewise, a SMA filter is implemented to extract pseudostatic responses from the rotation data containing both slow and fast dynamic components. Later, the extracted data are converted to pseudostatic displacement using simple Euler-Bernoulli beam formulations.

To evaluate and validate the estimation process, a realistic model of a timber bridge bent is simulated under different traffic conditions. In this model, the weight profile of a work train used for field testing is used as input to the simulation. Likewise, a sine wave is applied to the model to simulate the harmonic rock-and-roll motion of the train. Furthermore, to capture all dynamics of the bent during the train crossing, variations in the mass of the structure due to varying train loads are implemented. The resulting measured accelerations and rotations are fed to a real-time application to obtain the estimated displacements. Finally, these estimated responses are compared to the measured ones. It is observed that the proposed method reproduces realistic displacements with high fidelity. The results indicate that accurate transverse responses can be obtained under revenue service traffic in real time.

This proposed technique is especially useful for bridges susceptible to asymmetric loading that exhibit pseudostatic displacements. Although a variety of sensing techniques have been proposed in the past, the majority of those approaches either require expensive instrumentation or deliver a relatively inaccurate displacement measurement that ignores the pseudostatic component of the displacement, which is significant in railroad bridges. The proposed method fuses the acceleration and the rotation for the estimation of bridge displacement, which is less expensive and quicker than the previous approaches. Furthermore, this method may be run in real time, providing a rapid, informed decision to owners of railroad bridges.

CHAPTER 5. CONCLUSION AND FUTURE RESEARCH

This thesis has introduced a low-cost, battery-powered, efficient wireless intelligent sensor (LEWIS2), which is capable of collecting angular velocity and acceleration of different outdoor applications. The proposed sensing platform acquires data with a low-cost accelerometer, MPU9250. The performance of LEWIS2 sensing platform was validated through a series of field experiments.

The performance of LEWIS2 sensing platform was validated through a series of experiments.

The first experiment described in the thesis involved using LEWIS2 placed on a rocket that was launched into the air. The rocket was launched and at apogee the parachutes were deployed. After the rocket was retrieved, data acquisition on the sensor was stopped wirelessly using the XBee connected to a smartphone. The accelerations and angular velocities during takeoff and travel were correctly stored on the memory card. It was possible to record the acceleration and angular velocity during takeoff to provide the final estimate of the rocket trajectory.

The general purpose of this experiment was to demonstrate LEWIS2 is capable of working in environments with high vibration and displacements. This experiment also showed that LEWIS2 can measure angular velocity and acceleration to accurately estimate the trajectory of the rocket. More generally, this experiment has confirmed that LEWIS2 can be successfully applied in new disciplines such as aerospace engineering, whereas the obtained results provide new data that can be used to optimize the design of rockets.

The aim of the second experiment carried out in this thesis was to estimate transverse bridge displacements by aggregating data obtained from multiple reference-free sensors by minimally relying on the structural properties. This experiment replicated the one that was originally developed by Ozdagli et al. (2017), but instead of using commercial accelerometers the author of this thesis calculated the reference-free total displacement with the new LEWIS2 sensing platform. For this experiment, the author of this thesis used a cantilever column simulating the dynamic behavior of a timber railroad bridge pile. The column was placed over the shake table fixed to a rigid frame using an L-bracket and a damping pad. The author of this thesis placed two LEWIS2 platforms, one over the column and the other over the shake table. Subsequently an LVDT was installed, and the displacements measured by Moreu et al. (2015) were applied to the shake table. The acceleration and angular velocity data was collected from LEWIS2 and the displacements from the LVDT. The total displacements were obtained from the data collected by LEWIS2 and then compared with the LVDT. The obtained results show that LEWIS2 can measure reference-free transverse displacement with errors lower than 11%.

This thesis has also provided recommendations concerning future work that may further improve the characteristics and the application of LEWIS2. For instance, in order to enhance the reliability of LEWIS2 as an outdoor application, more experiments may be carried out to determine how the LEWIS2 sensor works in difficult environments for an extended period of time. The author of this thesis has completed a preliminary experiment of this type, which involved placing LEWIS2 in a tall tramway tower to test its performance and to measure the tower vibrations. The aim of such experiments is to support the capabilities for multiple field environments and structural responses of diverse infrastructures with low-cost, battery-powered, efficient wireless intelligent sensors. More generally, the overall objective of the research presented in this thesis is to enhance the reliability and accuracy of information that engineers receive about the performance of structures and installations, which lead to improvements in Structural Health Monitoring.

REFERENCES

AAR, A. o. (2013). *AAR 2013 Total Annual Spending Data. Retrieved from https://www.aar.org/Fact%20Sheets/Safety/2013-AAR_spending-graphic-fact-sheet.pdf.*

Adafruit. (2018). *Adafruit Powerboost 1000C. Product information retrieved from https://learn.adafruit.com/adafruit-powerboost-1000c-load-share-usb-charge-boost/overview.*

Akyildiz, I., Su, W., Sankarasubramaniam, Y., & Cayirci, E. (2002). *Wireless sensor networks: a survey.* Else Comput Netw 2002;38:393–422.

Arduino. (2018). *Arduino Uno Rev3. <https://www.arduino.cc/en/Guide/Environment> (July 26, 2018).*

AREMA, A. R.-o.-W. (2003). *Practical guide to railway engineering.* Lanham, MD.

AREMA, A. R.-o.-W. (2010). *Manual for railway engineering, Vol. 2.* Lanham, MD.

ASCE, A. S. (1988). *National Council on Public Works Improvement. Retrieved from https://www.infrastructurereportcard.org/wp-content/uploads/2017/03/1988-Fragile-Foundations-ExSum.pdf.*

ASCE, A. S. (1998). *1998 Report Card of America's Infrastructure. Retrieved from https://www.infrastructurereportcard.org/wp-content/uploads/2016/10/1998-ASCE-Report-Card-for-Americas-Infrastructure.pdf.*

ASCE, A. S. (2001). *2001 Report Card of America's Infrastructure. Retrieved from https://www.infrastructurereportcard.org/wp-content/uploads/2016/10/2001-ASCE-Report-Card-for-Americas-Infrastructure.pdf.*

ASCE, A. S. (2005). *2005 Report Card of America's Infrastructure. Retrieved from https://www.infrastructurereportcard.org/wp-content/uploads/2016/10/2005-ASCE-Report-Card-for-Americas-Infrastructure.pdf.*

ASCE, A. S. (2009). *2009 Report Card of America's Infrastructure. Retrieved from http://2013.infrastructurereportcard.org/2009/sites/default/files/RC2009_full_report.pdf.*

ASCE, A. S. (2013). *2013 Report Card of America's Infrastructure. Retrieved from http://2013.infrastructurereportcard.org/.*

ASCE, A. S. (2017). *Report Card of America's Infrastructure. Retrieved from https://www.infrastructurereportcard.org/wp-content/uploads/2016/10/Grades-Chart.png.*

Ashkenazi, V., & Roberts, G. (1997). *Experimental monitoring of the HumberBridgeusingGPS.* Proc.Inst.Civ.Eng.,120(4),177–182.

Atzeni, C., Bicci, A., Dei, D., Fratini, M., & Pieraccini, M. (2010). *Remote survey of the leaning tower of pisa by interferometric sensing.* IEEE Geoscience and Remote Sensing Letters, vol. 7, no. 1, pp. 185–189.

Bahrepour, M., Meratnia, N., Poel, M., Taghikhaki, Z., & Havinga, P. (2010). *Distributed event detection in wireless sensor networks for disaster management.* Thessaloniki, Greece: In Proceedings of the 2010 2nd International Conference on Intelligent Networking and Collaborative Systems (INCOS), pp. 507–512.

Bangali, J., & Shaligram, A. (2013). *Energy efficient Smart home based on Wireless Sensor Network using LabVIEW.* Am. J. Eng. Res. 2013, 2, 409–413.

Banzi, Massimo, & Shiloh, M. (2015). *Make: Getting Started with Arduino. Third edition.* Sebastopol, CA: Maker Media.

Bayo, A., Antolín, D., Medrano, N., Calvo, B., & Celma, S. (2010). *Early Detection and Monitoring of Forest Fire with a Wireless Sensor Network System.* Proced. Eng. 2010, 5, 248–251.

Bistrovs, V., & Kluga, A. (2012). *Adaptive extended Kalman filter for aided inertial navigation system.* Elektronika ir Elektrotechnika 122.6: 37-40.

Boller, C., Fou-Kuo, C., & Yozo, F. (2009). *Encyclopedia of Structural Health Monitoring.* Chichester, West Sussex, U.K.: John Wiley.

Brownjohn, J. W., De Stefano, A. X., Wenzel, H., & Aktan, A. E. (2011). *Vibration based monitoring of civil infrastructure: challengues and successes.* Journal of Civil Structural Monitoring 2(1), 79-95.

Cambridge Systematics, Inc. (2007). *National rail freight infrastructure capacity and investment study.* Cambridge, MA.

Cao, J., & Liu, X. (2012). *Structural health monitoring using wireless sensor networks, in Mobile and Pervasive Computing in Construction, C. J. Anumba and X. Wang.* Oxford, U.K.: Wiley, 2012, pp. 210–236.

Catbas, F., Kijewski-Correa, T., & Aktan, A. (2012). *Structural Identification of Constructed Facilities: Approaches, Methods, and Technologies for Effective Practice of StId, ASCE.* Reston, VA. USA.

Chang, P. C., Flatau, A., & Liu, S. C. (2003). *Health Monitoring of Civil Infrastructure.* Structural Health Monitoring 2.3, 257-267.

Chang, S. J., & Kim, N. S. (2012). *Estimation of displacement response from FBG strain sensors using empirical mode decomposition technique.* Exp.Mech.,52(6),573–589.

Chen, H. (2008). *Application of regularization method to damage detection in plane frame structures from incomplete noisy modal data.* Engineering Structures 30(11), 3219-3227.

Chen, H., & Bicanic, N. (2000). *Assessment of damage in continuum structures based on incomplete modal information.* Computers and Structures 74, 559-570.

Chen, H., & Maung, T. (2014). *Structural damage evolution assessment using regularized time step integration method.* Journal of Sound and Vibration 333(18), 4104–4122.

Chen, H.-P., & Ni, Y.-Q. (2018a). *Sensors and Sensing Technology for Structural Monitoring.*

Chen, H.-P., & Ni, Y.-Q. (2018b). *Structural Health Monitoring of Large Civil Engineering Structures.*

Chen, Q., Wang, L., & Zhao, H. (2009). *Hydrodynamic Investigation of Coastal Bridge Collapse during Hurricane Katrina.* Journal of Hydraulic Engineering 135.3, 175–186.

Chen, W. F., & Duan, L. (2014). *Bridge engineering handbook: Fundamentals, 2ndEd.* FL: CRCPress, BocaRaton.

Chintalapudi, K. et al. (2006). *Monitoring civil structures with a wireless sensor network.* IEEE Internet Comput., vol. 10, no. 2, pp. 26–34, Mar./Apr. 2006.

Cosser, E., Roberts, G., Meng, X., & Dodson, A. (2003). *Measuring the Dynamic Deformation of Bridges Using a Total Station. Proceeding of the 11th FIG Symposium on Deformation Measurements 25–28 May 2003.* Santorini, Greece.

Cranenbroeck, J. (2015). *Long Bridge GNSS Monitoring by CGEOS. Retrieved from: http://www.wallonia.be/en/blog/long-bridge-gnss-monitoring-cgeos.*

Cross, E., Worden, K., & Farrar, C. (2013). *Structural health monitoring for civil infrastructure. Health Assessment of Engineering Structures: Bridges and Other Infrastructure.* Singapore: Haldar (ed.), World Scientific Publishing.

Dai, K., Boyajian, D., Liu, W., Chen, S., Scott, J., & Schmieder, M. (2014). *Laser-based field measurement for a bridge finite-element model validation.* J. Perform. Constr. Facil., 10.1061/(ASCE)CF.1943-5509.0000484,04014024.

Davisson, M. T. (1970). *Lateral load capacity of piles.* Washington, DC: Highway Research Record No. 333, National Academy of Sciences-National Research Council.

Doebling, S., Farrar, C., Prime, M., & Shevitz, D. (1996). *Damage Identification and Health Monitoring of Structural and Mechanical Systems from Changes in their Vibration Characteristics: A Literature Review.* Los Alamos National Laboratory report LA-13070-MS.

Dunn, P., & Davis, M. (2018). *Measurement and Data Analysis for Engineering and Science. Fourth Edition. Boca Raton: CRC Press.*

Eamon, C. D., Fitzpatrick, P., & Truax, D. D. (2007). *Observations of Structural Damage Caused by Hurricane Katrina on the Mississippi Gulf Coast.* Journal of Performance of Constructed Facilities 21.2, 117–127.

Farrar, C., & Lieven, N. (2007). *Damage prognosis: the future of structural health monitoring.* Philosophical Transactions of the Royal Society A 365, 623–632.

Farrar, C., & Worden, K. (2007). *An introduction to structural health monitoring. Philosophical Transactions of the Royal Society Series A 365: 303-315.*

Farrar, C., Sohn, H., Hemez, F., Anderson, M., Bement, M., Cornwell, P., . . . J.F., S. (2003). *Damage Prognosis: Current Status and Future Needs.* Los Alamos National Laboratory report LA-14051-MS.

Farrar, C., Worden, K., & Dulieu-Barton, J. (2009). *Principles of structural degradation monitoring. Encyclopaedia of Structural Health Monitoring.* Chichester, UK: Boller, Chang and Fujino (ed.), John Wiley & Sons.

Feng, D., Feng, M. Q., Ozer, E., & Fukuda, Y. (2015a). *A vision-based sensor for noncontact structural displacement measurement.* Sensors, 15(7),16557–16575.

Feng, M., Fukuda, Y., Feng, D., & Mizuta, M. (2015b). *Nontarget vision sensor for remote measurement of bridge dynamic response.* J. Bridge Eng.,04015023.10.1061/(ASCE)BE.1943-5592.0000747.

Figliola, R., & Beasley, D. (2010). *Theory and Design for Mechanical Measurements. 5th Edition. Hoboken, NJ: John Wiley & Sons. .*

Fischer, C., Poorna, T. S., & Hazas, M. (2013). *Tutorial: implementation of a pedestrian tracker using foot-mounted inertial sensors.* IEEE pervasive computing 12.2: 17-27.

Fisher, C. J. (2010). *AN-1057 application note: Using an accelerometer for inclination sensing. http://www.analog.com/media/en/technical-documentation/application-notes/AN-1057.pdf. (Jun. 1, 2017).*

FRA, F. R. (2008). *Railroad bridge working group reporttothe railroad safetyadvisory committee. https://rsac.fra.dot.gov/document.php?type=meeting&date=20.* Washington, DC: Railroad Bridge Working Group Final Rep.

FRA, F. R. (2016). *Freight rail today. https://www.fra.dot.gov/Page/P0362 (Aug.4,2016).*

Frangopol, D., & Messervey, T. (2009). *Maintenance Principles for Civil Structures. Encyclopedia of Structural Health Monitoring.* Chichester, UK: Boller, Chang and Fujino (ed.), John Wiley & Sons.

Fukuda, Y., Feng, M., & Shinozuka, M. (2010). *Cost-effective vision-based system for monitoring dynamic response of civil engineering structures.* Struct.ControlHealthMonit.,17(8),918–936.

Garg, P. (2018). *Displacement Measurement Using a Laser Doppler Vibrometer Mounted on an Unmanned Aerial Vehicles. Master thesis, University of New Mexico. http://digitalrepository.unm.edu/ece_etds/402.*

Gavin, H. P., Rodrigo, M., & Kathryn, R. (1998). *Drift-free integrators.* Rev.Sci.Instrum.,69(5),2171–2175.

Handcock, R., Swain, D., Bishop-Hurley, G., Patison, K., Wark, T., & Valencia, P. (2009). *Monitoring Animal Behaviour and Environmental Interactions Using Wireless Sensor Networks, GPS Collars and Satellite Remote Sensing.* Sensors 2009, 9, 3586–3603.

Helmi, K., Taylor, T., Zarafshan, A., & Ansari, F. (2015). *Reference free method for real time monitoring of bridge deflections.* Eng. Struct., 103,116–124.

Hou, X., Yang, X., & Huang, Q. (2005). *Using inclinometers to measure bridge deflection.* J. BridgeEng., 10.1061/(ASCE)1084-0702(2005)10:5(564),564–569.

IBISWorld. (2016). *Rail transportationintheUS:Market researchreport. http://www.ibisworld.com/industry/default.aspx?indid=1133 (Aug. 4,2016).*

Invensense. (2018). *MPU-9250 Product Specification Document Number: PS-MPU-9250A-01 Revision: 1.1 Release Date: 06/20/2016. Retrieved from https://www.invensense.com/wp-content/uploads/2015/02/PS-MPU-9250A-01-v1.1.pdf.*

Jiang, P., Xia, H., He, Z., & Wang, Z. (2009). *Design of a Water Environment Monitoring System Based on Wireless Sensor Networks.* Sensors 2009, 9, 6411–6434.

Jo, B.-W., Yun-Sung, L., Jun, H. J., Rana, M., & Asad, K. (2018). *Computer Vision-Based Bridge Displacement Measurements Using Rotation-Invariant Image Processing Technique.* Sustainability, vol. 10(6), pages 1-16.

Karbhari, M. (2009). *Design principles for civil structures. Encyclopaedia of Structural Health Monitoring.* Chichester, UK: Boller, Chang and Fujino (ed.), John Wiley & Sons.

Kim, K., & Sohn, H. (2017). *Dynamic displacement estimation by fusing LDV and LiDAR measurements via smoothing based Kalman filtering.* Mech.Syst.Sig.Process.,82,339–355.

Kim, N. S., & Cho, N. S. (2004). *Estimating deflection of a simple beam model using fiber optic Bragg-grating sensors.* Exp. Mech., 44(4), 433–439.

Ko, J., & Ni, Y. (2005). *Technology developments in structural health monitoring of large-scale bridges.* Engineering Structures 27(12), 1715-1725.

Kogan, M. G., Kim, W. Y., Bock, Y., & Smyth, A. W. (2008). *Load response on a large suspension bridge during the NYC Marathon revealed by GPS and accelerometers.* Seismological Research Letters, 79(1), 12-19.

Lacono, M., Romano, E., & Marrone, S. (2010). *Adaptive monitoring of marine disasters with intelligent mobile sensor networks.* Taranto, Italy: In Proceedings of the 2010 IEEE Workshop on Environmental Energy and Structural Monitoring Systems (EESMS), pp. 38–45.

Lai, Y. C. (2008). *Increasing railway efficiency and capacity through improved operations, control and planning.* Univ. of Illinois at Urbana–Champaign, Champaign, IL.

Lee, H., Banerjee, A., Fang, Y., Lee, B., & King, C. (2010). *Design of a multifunctional wireless sensor for in situ monitoring of debris flows.* IEEE Trans. Instrum. Meas. 2010, 59, 2958–2967.

Lee, H., Hong, Y., & Park, H. (2010). *Design of a FIR filter for the displacement reconstruction using measured acceleration in low-frequency dominant structures.* Int. J. Numer. Methods Eng. 82 (4) (2010) 403–434.

Lee, H., Wu, C., & Aghajan, H. (2011). *Vision-based user-centric light control for smart environments.* Pervasive Mob. Comput. 2011, 7, 223–240.

Lee, J. J., & Shinozuka, M. (2006a). *A vision-based system for remote sensing of bridge displacement.* NDTEInt.,39(5),425–431.

Lee, J. J., & Shinozuka, M. (2006b). *Real-time displacement measurement of a flexible bridge using digital image processing techniques.* Exp.Mech.,46(1),105–114.

Li, X., Deng, Y., & Ding, L. (2008). *Study on precision agriculture monitoring framework based on wsn. In Proceedings of the 2nd International Conference on Anti-counterfeiting, Security and Identification (ASID 2008).* Guiyang, China: pp. 182–185.

Ligorio, G., & Sabatini, A. M. (2013). *Extended Kalman filter-based methods for pose estimation using visual, inertial and magnetic sensors: Comparative analysis and performance evaluation.* Sensors 13.2: 1919-1941.

Lynch, J. P. (2012). *Long-Term Wireless Monitoring Systems for the Monitoring of Long-span Bridges.* Paper presented at the 2012 Michigan Bridge Conference Howell, Michigan, March 21, 2012.

Lynch, J. P., & Loh, K. (2006). *A Summary Review of Wireless Sensors and Sensor Networks for Structural Health Monitoring.* The Shock and Vibration Digest 38.2, 91–128.

Mehrabi, A. (2006). *In-service evaluation of cable-stayed bridges, overview of available methods and findings.* Journal of Bridge Engineering, 11(6), 716-724.

Meng, X., Dodson, A. H., & Roberts, G. W. (2007). *Detecting bridge dynamics with GPS and triaxial accelerometers.* Eng. Struct., 29(11), 3178–3184.

Moreu, F. (2015). *Framework for risk-based management and safety of railroad (Doctoral dissertation, University of Illinois at Urbana-Champaign).*

Moreu, F., & et al. (2015). *Dynamic assessment of timber railroad bridges using displacements.* J. Bridge Eng, 10.1061/(ASCE)BE.1943-5592.0000726,04014114.

Moreu, F., & LaFave, J. M. (2012). *Current research topics: Railroad bridges and structural engineering.* Champaign, IL: Newmark Structural Engineering Laboratory, Univ. of Illinois at Urbana–Champaign.

Moreu, F., H., J. L., Jo, R. K., Scola, S., Spencer Jr., B., & LaFave, J. (2015). *Reference-free displacements for condition assessment of timber railroad bridges.* J. Bridge Eng. (2015), https://doi.org/10.1061/(ASCE)BE.1943-5592.0000805, 04015052.

Moreu, F., Jo, H., Li, J., Kim, R., Cho, S., Kimmle, A., & LaFave, J. (2014). *Dynamic assessment of timber railroad bridges using displacements.* Journal of Bridge Engineering, 20(10), 04014114.

Moreu, F., Kim, R. E., & Spencer, B. F. (2017). *Railroad bridge monitoring using wireless smart sensors.* Struct. Control Health Monit., 24, e1863.

Moreu, F., Spencer, B. F., Foutch, D. A., & Scola, S. (2017). *Consequence-based management of railroad bridge networks.* Struct. Infrastruct.Eng.,13(2),273–286.

Moschas, F., & Stiros, S. (2011). *Measurement of the dynamic displacements and of the modal frequencies of a short-span pedestrian bridge using GPS and an accelerometer.* Eng.Struct.,33(1),10–17.

Moschas, F., Psimoulis, P. A., & Stiros, S. C. (2013). *GPS/RTS data fusion to overcome signal deficiencies in certain bridge dynamic monitoring projects.* Smart Structures and Systems, 12(3.4), 251-269.

Nadimi, E., Jørgensen, R. B.-V., & Christensen, S. (2012). *Monitoring and classifying animal behavior using ZigBee-based mobile ad hoc wireless sensor networks and artificial neural networks.* Comput. Electron. Agric. 2012, 82, 44–54.

Nakamura, S. (2000). *GPS measurement of wind-induced suspension bridge girder displacements.* J. Struct. Eng., 10.1061/(ASCE)0733-9445(2000)126:12(1413),1413–1419.

Nanotech. (2018). *Turnigy nano-tech 1000mah 2S 25~50C Lipo Pack. Product information retrieved from https://hobbyking.com/en_us/turnigy-nano-tech-1000mah-2s-25-50c-lipo-pack.html?___store=en_us .*

Nassif, H. H., Gindy, M., & Davis, J. (2005). *Comparison of laser Doppler vibrometer with contact sensors for monitoring bridge deflectionandvibration.* NDTEInt.,38(3),213–218.

Ni, Y. (2014). *Sensing Solutions for Assessing and Monitoring Supertall Towers. In book: Sensor Technologies for Civil Infrastructures (Vol. 2): Applications in Structural Health Monitoring.* Cambridge, UK: Wang, Lynch and Sohn (ed.), Woodhead Publishing.

Noel, A., Abdaoui, A., Badawy, A., Elfouly, T., Ahmed, M., & Shehata, M. (2017). *Structural Health Monitoring using Wireless Sensor Networks: A Comprehensive Survey.* IEEE Commun. Surv. Tutor. 2017, 19, 1403–1423.

OCIA, D. N. (2016). *Critical Infrastructure Security and Resilience Note: Aging and Failing Infrastructure Systems: Highway Bridges. Retrieved from: https://www.dhs.gov/.*

Olaszek, P. (1999). *Investigation of the dynamic characteristic of bridge structures using a computer vision method.* Measurement, 25(3), 227–236.

Ozdagli, A. I., Gomez, J. A., & Moreu, F. (2017). *Real-time reference-free displacement of railroad bridges during train-crossing events.* J. Bridge Eng., 10.1061/(ASCE)BE.1943-5592.0001113, 04017073.

Ozdagli, A., Liu, B., & Moreu, F. (2018). *Low-cost, efficient wireless intelligent sensors (LEWIS) measuring real-time reference-free dynamic displacements.* Mechanical Systems and Signal Processing 107 (2018) 343–356.

Padgett, J., DesRoches, R., Nielson, B., Yashinsky, M., Kwon, O.-S., Burdette, N., & Tavera, E. (2008). *Bridge Damage and Repair Costs from Hurricane Katrina.* Journal of Bridge Engineering 13.1: 6–14.

Padmavathi, G., Shanmugapriya, D., & Kalaivani, M. (2010). *A Study on Vehicle Detection and Tracking Using Wireless Sensor Networks. Wirel. Sens. Netw.* Sensors 2014, 14 16950.

Park, J. W., Lee, K. C., Sim, S. H., Jung, H. J., & Spencer, B. F. (2016). *Traffic safety evaluation for railway bridges using expanded multisensor data fusion.* Comput.-Aided Civil Infrastruct. Eng. 31 (10) (2016) 749–760.

Park, J. W., Sim, S. H., & Jung, H. J. (2014). *Wireless displacement sensing system for bridges using multi-sensor fusion, Smart Mater.* Struct. 23 (4) (2014) 045022.

Perez, C., Jimenez, M., Soto, F., Torres, R., López, J., & Iborra, A. (2011). *A system for monitoring marine environments based on Wireless Sensor Networks.* Santander, Spain: In Proceedings of the IEEE Conference on OCEANS pp. 1–6.

Pieraccini, M. (2013). *Monitoring of Civil Infrastructures by Interferometric Radar: A Review.* The Scientific World Journal, Volume 2013, Article ID 786961, http://dx.doi.org/10.1155/2013/786961.

Pieraccini, M., Fratini, M., Parrini, F., Pinelli, G., & Atzeni, C. (2005). *Dynamic survey of architectural heritage by high-speed microwave interferometry.* IEEE Geoscience and Remote Sensing Letters, vol. 2, no. 1, pp. 28–30, 2005.

Pieraccini, M., Parrini, F., Fratini, M., Atzeni, C., Spinelli, P., & Micheloni, M. (2006). *Static and dynamic testing of bridges through microwave interferometry.* NDT&E International 40 (2007) 208–214.

Polytec Inc. (2017). *"Technical Data." OFV-534 Compact Sensor Head. Retrieved from http://www.polytec.com/fileadmin/user_uploads/Products/Vibrometers/OFV-534/Documents/OM_DS_OFV-534_E_42367.pdf.*

Psimoulis, P., & Stiros, S. (2013). *Measuring deflections of a short-span railway bridge using a robotic total station.* J. Bridge Eng., 10.1061/(ASCE)BE.1943-5592.0000334,182–185.

Psimoulis, P., Stella, P., Dimitris, K., & Stathis, S. (2008). *Potential of Global Positioning System (GPS) to measure frequencies of oscillations of engineering structures.* Journal of Sound and Vibration Volume 318, Issue 3, 9 December 2008, Pages 606-623 https://pdfs.semanticscholar.org/ea71/43fa0e3d773d806a4c8a1e2b6e9dd797ac2f.pdf .

Puente, I., Solla, M., González-Jorge, H., & Arias, P. (2015). *NDT documentation and evaluation of the Roman Bridge of Lugo using GPR and mobile and static LiDAR.* J. Perform. Constr. Facil., 10.1061/(ASCE)CF.1943-5509.0000531,06014004.

Qian, H., Sun, P., & Rong, Y. (2012). *Design Proposal of Self-Powered WSN Node for Battle Field Surveillance.* Energy Proced. 2012, 16, 753–757.

Raul, M., Samuel, G., Miguel, A., António, L., Salviano, F., Ferreira, P., & Reis, M. (2008). *Sun, wind and water flow as energy supply for small stationary data acquisition platforms.* Comput. Electron. Agric. 2008, 64, 120–132.

Ribeiro, D., Calçada, R., Ferreira, J., & Martins, T. (2014). *Non-contact measurement of the dynamic displacement of railway bridges using an advanced video - based system.* Eng.Struct.,75,164–180.

Sanli, A., Uzgider, E., Caglayan, O., Ozakgul, K., & Bien, J. (2000). *Testing bridges by using tiltmeter measurements.* Transp. Res. Rec., 1696,111–117.

Silkorsky, C. (1999). *Development of a Health Monitoring System for Civil Structures using a Level IV Non-Destructive Damage Evaluation Method, Proceedings of the 2nd International Workshop on Structural Health Monitoring.* Stanford, CA, USA.

Silva, I., Guedes, L., Portugal, P., & Vasques, F. (2012). *Reliability and Availability Evaluation of Wireless Sensor Networks for Industrial Applications.* Sensors 2012, 12, 806–838.

Smyth, A., & Wu, M. (2007). *Multi-rate Kalman filtering for the data fusion of displacement and acceleration response measurements in dynamic system monitoring.* Mech. Syst. Sig. Process., 21(2), 706–723.

Sohn, H., Farrar, C., Hemez, F., Shunk, D., Stinemates, D., & Nadler, B. (2004). *A Review of Structural Health Monitoring Literature: 1996–2001.* Report LA-13976-MS. Los Alamos National Laboratory.

Spencer, J. B., Sandoval, M. E., & Kurata, N. (2004). *Smart Sensing Technology: Opportunities and Challenges.* Journal of Structural Control and Health Monitoring 11.4, pp. 349–368.

Stiros, S. C., & Psimoulis, P. A. (2012). *Response of a historical short-span railway bridge to passing trains: 3-D deflections and dominant frequencies derived from robotic total station (RTS) measurements.* Eng. Struct.,45,362–371.

Surface Transportation Board. (2016). *FAQs. https://www.stb.gov/stb/faqs.html (Aug.4,2016).*

Sutton, G. P., & Biblarz, O. (2010). *Rocket Propulsion Elements.*

Tacconi, D., Miorandi, D., Carreras, I., Chiti, F., & Fantacci, R. (2010). *Using wireless sensor networks to support intelligent transportation systems.* Ad Hoc Netw. 2010, 8, 462–473.

TRB, T. R. (2006). *Maintenance and operations of transportation facilities.* Washington, DC: Transportation Research Circular E-C092.

Tubaishat, M., Zhuang, P., Qi, Q., & Shang, Y. (2009). *Wireless sensor networks in intelligent transportation systems. .* Wirel. Commun. Mob. Comput. 2009, 9, 287–302.

Voltaic. (2018). *Medium 6V 2W Solar panel - 2.0 Watt from Voltaic Systems. Product information retrieved from https://www.adafruit.com/product/200.*

Wahbeh, A., Caffrey, J., & Masri, S. (2003). *A vision-based approach for the direct measurement of displacements in vibrating systems. Smart Mater. Struct. 2003, 12, 785.*

Wang, M. L., Lynch, J. P., & Sohn, H. (2014). *Sensor Technologies for Civil Infrastructures, Volume 1: Sensing Hardware and Data Collection Methods for Performance Assessment. Woodhead Publishing Series in Electronic and Optical Materials.* Amsterdam: Woodhead Publishing.

Watson, C., Watson, T., & Coleman, R. (2007). *Structural monitoring of cable-stayed bridge: Analysis of GPS versus modeled deflections.* J. Surv. Eng., 10.1061/(ASCE)0733-9453(2007)133:1(23), 23–28.

Wipf, T., Ritter, M., & Wood, D. (2000). *Evaluation and field load testing of timber railroad bridge.* Transp. Res. Rec., 1696, 323–333.

Wong, K. Y. (2004). *Instrumentation and health monitoring of cable-supported bridges.* Struct.Contr.HealthMonit.,11(2),91–124.

Wong, K. Y., Man, K. L., & Chan, W. Y. (2001). *Real-time kinematic spansthegap.* GPSWorld,12(7),10–19.

Wong, K., & Ni, Y. (2009). *Modular architecture of structural health monitoring system for cable-supported bridges. Encyclopaedia of Structural Health Monitoring.* Chichester, UK: Boller, Chang and Fujino (ed.), John Wiley & Sons.

XBee Explorer. (2018). *SparkFun XBee Explorer USB. Product information retrieved from https://www.sparkfun.com/products/11812.*

XBee, D. (2018). *Digi XBee® Family Features Comparison. Retrieved from https://www.digi.com/pdf/chart_xbee_rf_features.pdf (July 28, 2018).*

Yi, T. H., Li, H. N., & Gu, M. (2013). *Experimental assessment of high-rate GPS receivers for deformation monitoring of bridge.* Measurement, 46(1),420–432.

Yunus, E., Ibrahim, K., & Özgür, U. (2012). *A framework for use of wireless sensor networks in forest fire detection and monitoring.* Comput. Environ. Urban Syst. 2012, 36, 614–625.

Zhao, G. (2011). *Wireless Sensor Networks for Industrial Process Monitoring and Control: A Survey.* Netw. Protoc. Algorithms 2011, 3, 46–63.

Zhi, R. (2016). *A Drift Eliminated Attitude & Position Estimation Algorithm In 3D. Graduate College Dissertations and Theses. Paper 450, University of Vermont.*

UNIVERSITAT POLITÈCNICA DE VALÈNCIA

ESCUELA TÉCNICA SUPERIOR INGENIEROS INDUSTRIALES VALENCIA

I undersigned, FERNANDO MOREU, PhD, PE member of teaching staff at the department/school/faculty of Civil, Construction and Environmental Engineering at University of New Mexico, certify that the exchange student Marlon Agüero Infante coming from Escuela Técnica Superior de Ingenieros Industriales (ETSII), Universitat Politècnica de València (Spain), has developed an independent undergraduate work, equivalent for his/her home university to a bachelor/master thesis, in the academic year 2017-18, with the title:

CONDITION ASSESSMENT OF CRITICAL INDUSTRIAL INFRASTRUCTURE WITH LOW-COST, EFFICIENT WIRELESS INTELLIGENT SENSORS (LEWIS)

The project was presented orally in ENGLISH [language] on 05/25/2018 and assessed by a jury.

The grade obtained was A WITH DISTINCTIONS

In Albuquerque, NM, on 05/25/2018

Prof. FERNANDO MOREU, PE, PhD

[Signature and stamp]

THE UNIVERSITY OF NEW MEXICO · 1889 ·